applied sciences

MDPI

Review

The Use of Supercontinuum Laser Sources in Biomedical Diffuse Optics: Unlocking the Power of Multispectral Imaging

Frédéric Lange [1,*], Luca Giannoni [1,2,3] and Ilias Tachtsidis [1]

[1] Biomedical Optics Research Laboratory, Department of Medical Physics and Biomedical Engineering, University College London, London WC1E 6BT, UK; giannoni@lens.unifi.it (L.G.); i.tachtsidis@ucl.ac.uk (I.T.)
[2] National Institute of Optics, National Research Council, 50019 Sesto Fiorentino, Italy
[3] European Laboratory for Non-linear Spectroscopy, 50019 Sesto Fiorentino, Italy
* Correspondence: f.lange@ucl.ac.uk

Abstract: Optical techniques based on diffuse optics have been around for decades now and are making their way into the day-to-day medical applications. Even though the physics foundations of these techniques have been known for many years, practical implementation of these technique were hindered by technological limitations, mainly from the light sources and/or detection electronics. In the past 20 years, the developments of supercontinuum laser (SCL) enabled to unlock some of these limitations, enabling the development of system and methodologies relevant for medical use, notably in terms of spectral monitoring. In this review, we focus on the use of SCL in biomedical diffuse optics, from instrumentation and methods developments to their use for medical applications. A total of 95 publications were identified, from 1993 to 2021. We discuss the advantages of the SCL to cover a large spectral bandwidth with a high spectral power and fast switching against the disadvantages of cost, bulkiness, and long warm up times. Finally, we summarize the utility of using such light sources in the development and application of diffuse optics in biomedical sciences and clinical applications.

Keywords: supercontinuum laser; NIRS; tissue optics; diffuse optics

Citation: Lange, F.; Giannoni, L.; Tachtsidis, I. The Use of Supercontinuum Laser Sources in Biomedical Diffuse Optics: Unlocking the Power of Multispectral Imaging. *Appl. Sci.* **2021**, *11*, 4616. https://doi.org/10.3390/app11104616

Academic Editor: Byoung-Kwan Cho

Received: 11 April 2021
Accepted: 7 May 2021
Published: 18 May 2021

1. Introduction

Non-invasive optical monitoring of the human physiology has been a great asset in the medical diagnosis over the last decades [1], and this field is still expanding as technological advances drives the development of new instruments for use in various medical applications [2]. One of the main techniques of optical monitoring of biological tissues is near-infrared spectroscopy (NIRS). It is based on the use of light between 650 and 900 nm, which is within the so-called "transparency window". Within this light window, the optical absorption of biological tissue is at its lowest and light scattering is sufficiently high so the propagation of light in tissue is facilitated. Therefore, NIRS provides a way to gather information from deep into the tissue [3]. As one of the main absorbers in this window is the hemoglobin, in its oxygenated and deoxygenated forms (oxy- and deoxy-hemoglobin ([HbO_2] and [HHb], respectively), NIRS has been broadly used to quantify the changes in oxygenation of various tissues like muscle and brain [4]. This ability to quantify oxygenation non-invasively, and in real time has helped NIRS to become a standard technique in the labs. However, a few pitfalls are still holding back its wide adoption at a clinical level. Indeed, most of the widespread techniques used for NIRS are based on the so-called continuous wave (CW) technique where the tissue is illuminated with a non-coherent light and the variation in light intensity is collected at the detector [5]. In this configuration, it is harder to estimate absolute quantities, as the underlying optical properties of the tissue (mainly absorption and scattering coefficient) cannot be measured, and the scattering properties are assumed to be fixed (i.e., in time and for every subject). Therefore, most of the CW-NIRS systems only quantify the changes in hemoglobin concentration. This can be a drawback for clinical use, as an absolute comparison between two patients

cannot be done unless you involve a well-controlled physiological stimulus. The other drawback is that the measurement is often performed with only two wavelengths, the minimum necessary to retrieve two absorbing compounds [HbO_2] and [HHb]. However, the contribution of other chromophores is either neglected (like collagen), or assumed and fixed, like water. This results in an increase in the physiological noise, which reduces the accuracy of the measurement.

These drawbacks have been tackled over the recent years, and some new techniques and instrumentation enabled researchers to work around these drawbacks. Firstly, one can use more advanced CW-NIRS techniques in order to extract absolute information about the tissue. We can cite the broadband NIRS that also has the capability to extract absolute information of tissue optical properties [6]. The added benefits of this technique are that, as it uses a large number of wavelength (typically more than a hundred), it can perform a true spectroscopic analysis, hence also gathering information about other chromophores like cytochromes, water, and fat [6]. This extra information enables having a complete optical view of the tissue under investigations. Moreover, on top of providing a more precise view of the oxygenation, the use of many wavelengths enables targeting novel optical contrasts, like the oxidative state of the cytochrome-c-oxidase (oxCCO) which is a biomarker of metabolism [7].

However, even though these improvements are promising, performing a true spectroscopic measurement on tissue using NIRS is still challenging. One of the main issues is the penetration depth of the light and the contamination of the tissues of interest by the upper layers (i.e., skin) [3]. Indeed, the tissues are often modelled as homogeneous for simplicity, even though this hypothesis is not true. Therefore, new methodologies are required to enhance the discrimination between different tissue types, thus improving the accuracy of the measurement.

It is well known that the time-domain NIRS (TD-NIRS) is the most advanced and accurate type of measurement, capable of retrieving absolute information and to discriminate between shallow and deep tissue [8]. Briefly, in TD-NIRS an ultra-short light impulse (typically in the picosecond range) illuminates the tissue. Tissue has the effect of attenuating and broadening the re-emitted pulse (the resulting pulse-width is typically few nanoseconds wide). The measured signal is typically called a temporal point spread function (TPSF) or distribution of time of flights (DTOFs) of photons. Indeed, what is measured here is the histogram of the arrival time of photons. Thus, the amount of information acquired by TD-NIRS systems outstrips the classical CW-NIRS, which only acquires the intensity. From these DTOF, various data processing methods can be employed to extract information about the tissue. It is out of the scope of this paper to detail these methods, but the interested reader can refer to the following reviews for a more in-depth description of TD-NIRS methodologies [9,10], and for a special focus on broadband TD-NIRS [11], which will be largely discussed in the present work.

The extraction of more accurate information with TD-NIRS comes at the cost of a more complex instrumentation, requiring pulsed-laser source (pulse in order of MHz) and fast electronic and sensitive detectors in order to be able to unlock single photon counting. Thus, even though TD-NIRS has been around for many decades now and has been developed in parallel to CW-NIRS, these more specific requirements have hindered its development. Nevertheless, much progress has been made over the last two decades, and TD-NIRS is closing the gap with CW-NIRS in terms of user's adoption.

One of the key developments that has promoted the development of TD-NIRS is the supercontinuum laser (SCL) sources, which provide a white laser source, with a high power (several watts) and a very short pulse width (typical less than 10 ps) at several tens of MHz. Indeed, these characteristics are essential in order to develop reliable TD-NIRS systems, that started to be developed in the nineties. During these early days of development, no commercial pulsed laser diodes were available, and one had to rely on homemade SC generation or Ti-Sapphire lasers in order to be able to produce a coherence pulsed light with a spectral power density sufficient to be detected by the photon counting electronic.

Therefore, SCL sources have been a true driver of TD-NIRS development in the early days, and have more recently unlocked new horizons like spectroscopy, which have broadened the fields of applications.

Finally, besides traditional sparse measurement of tissue properties with diffuse optics, Diffuse Optical Tomography (DOT) has also been rapidly expending in the past decades. This imaging technique is based on the acquisition of a large number of channels, coupled to a more refined data analysis, based on anatomically realistic models of tissue. This allows to reconstruct 3D spatial distribution of optical/physiological parameters of the tissues, rather than providing tissue information on a limited number of points. An extension of this technique is called fluorescence DOT, that uses extrinsic near-infrared fluorescent dyes which targets specific tissues to harvest extra information and enable molecular imaging. The interested reader can refer to reviews [12,13] for more information about these techniques. We will see that SCL sources have also a role to play in order to improve the performances of the DOT instruments.

In this work, we will review the use of SCL in the field of biomedical diffuse optics. Thus, we will begin by a short overview of the history and basic principle of supercontinuum generation. Then, we will review works that have been using SCL in biomedical diffuse optics, from the instrument development to the application. Finally, we will summarize and highlight the strength and weakness of SCL for these applications and show what areas can benefits from its use.

2. History and Basic Principles of Supercontinuum Lasers

Supercontinuum (SC) lasers are broadband, coherent light sources that are capable of combining the wide spectral range of conventional white lamps (including UV, visible and IR light) with the optical performances of single-mode lasers, in particular their high output intensity, the capability of fast, pulsed emission, and the fine collimation of the beam down to diffraction limit. Such characteristics make this type of photonic technology highly versatile for a number of applications, in particular in biomedical optics and biophotonics, thanks also to recent advancement towards making SC lasers more compact and affordable [14].

The physical process of optical SC generation was discovered and studied in the 60 s and 70 s with milestones publications by Alfano and Shapiro [15,16]. It is based on the propagation of extreme non-linear effects from a narrow-bandwidth pulsed laser beam in order to generate a broadening of the overall spectrum of the emitted light. These non-linear effects typically include self-phase modulation, four-wave mixing, Raman scattering, and solitons dynamics, among others [14,17]. The propagation of these effects is performed by dispersing the pulsed laser beam through a non-linear material. These can range from bulk materials, such as simple water cells, silicas, or gases (as in the earliest attempts of SC generation), to more advanced crystal-structured optical fibres [17,18].

Early SC lasers using bulk materials for non-linear propagation were limited in the efficiency of coupling the input laser light with these propagating material (coupling efficiencies stood at below 10%) and thus they were able to only achieve ranges of about 200–300 nm, with pulses duration in the order of tens of nanoseconds. Further developments in SC generation efficiency and coupling using optic fibres lead to enlarging the range up to 1–2 µm and increasing the pulse duration to the range of picoseconds (for commercial, compact lasers), or even femtoseconds (for research-grade, benchtop lasers) [18]. A critical turning point for modern SC lasers to achieve such high performances was the invention and application of photonic crystal fibres (PCF), a particular type of microstructured optic fibre (Figure 1).

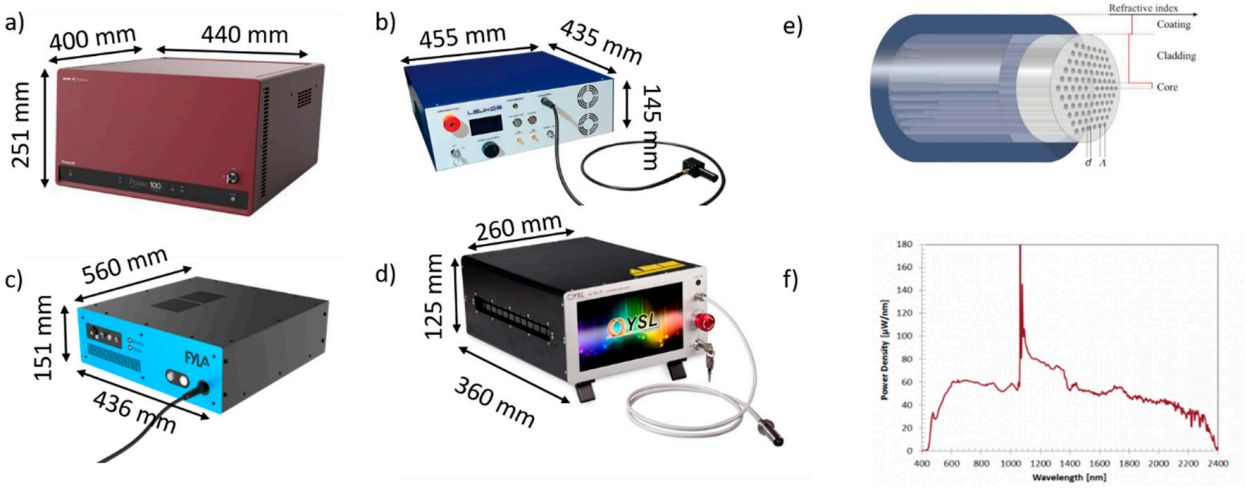

Figure 1. Example of commercial SC laser sources and their typical spectra. (**a**) Fianium source, (**b**) Leukos source, (**c**) FYLA source, (**d**) YSL source. (**e**) Schematic of the classical triangular cladding single-core photonic crystal fiber in which light is guided in a solid core embedded in a triangular lattice of air holes. The fiber structure is determined by the hole-size, d, and the hole-pitch, Λ. Like standard fibers, the PCF is coated with a high index polymer for protection and to strip off cladding-modes. Extracted from the application note on supercontinuum generation in photonic crystal fibers by NKT. (**f**) Example of full spectrum generated by a SC laser, showing the width of the broadband emission and the central peak wavelength that is a residual of the single-mode laser used for SC generation. The spectrum is taken from the SuperK COMPACT SC laser manufactured by NKT Photonics (https://www.nktphotonics.com/lasers-fibers/product/superk-compact-supercontinuum-lasers/, accessed date: 1 November 2021).

PCFs, invented in 1996 [19], are currently the most used non-linear propagating materials for SC generation [17,18]. As the name suggests, this class of optic fibres is based on recreating the optical properties of crystalline structures, in particular their photonic bandgap effect, by combining various high and low refractive indexes in their inner structure. Such features can be achieved in different manners, which typically define the given category of PCFs [20]: (1) hollow-core PCFs present a central hole in their structures, filled with air; (2) holey PCFs are composed of a matrix of several air-filled holes in their cross-sections that is interspersed with the core material; (3) solid-core PCFs involves a solid core surrounded by a matrix of air-filled holes.

PCFs offer high coupling efficiencies and low power losses, thus allowing ultra-broadband, high-brightness SC generation at cost-effective access [17,21]. SC lasers based on PCFs used in biomedical optics applications can typically generate broad spectrum spanning from 350 to 2400 nm, generally showing a central sharp peak which is a residual of the original shape of the pulsed beam. An example of this is shown in Figure 1. Most commercial SC lasers show performances similar to pulsed laser diodes, with integrated output power up to tens of watts and the capability of generating pulses in the order of picoseconds and repetition rates of tens of MHz [22].

Finally, we can report that in the recent year, more companies are able to provide ready-to-use SC solution. A search from the website https://www.rp-photonics.com (accessed date: 1 November 2021), displays at least 4 companies manufacturing SCL: NKT photonics, who recently acquired the former UK company Fianium (www.nktphotonics.com, accessed date: 1 November 2021), LEUKOS (www.leukos-systems.com, accessed date: 1 November 2021), FYLA (www.fyla.com, accessed date: 1 November 2021) and YSL photonics (www.yslphotonics.com, accessed date: 1 November 2021). Figure 1 displays pictures of different SCL offered by these companies.

3. The Use of Supercontinuum Lasers in Biomedical Diffuse Optics

The focus of the present review was to evaluate the use of SCL in biomedical diffuse optics, from the systems and methodological developments to their medical applications.

Therefore, papers were identified using PubMed, Scopus, and Web of Science, searching for a combination of keywords including (supercontinuum laser | white laser) and (diffuse optics | NIRS). Moreover, a manual search from articles' references was performed and the personal reference library of the authors of the current papers has also been searched. Papers were rejected if no SCL was used in the method section of the reported work, if the application was not medically related, if they were reviews or if the method was not purely optical (i.e., no photoacoustic papers). A total of 95 publications covering a variety of focus were identified. We have identified 4 main categories of publications: system development (31 studies), optical properties estimation (16 studies), methodology (43 studies) and application (5 studies). Table 1 provides a summary of the main characteristics of the SCL used in the studies reported in this review, Figure 2 shows pictures of the instrumentation typically used, and Figure 3 presents typical output in terms of datatypes of such systems. Moreover, a summary of the studies included in this review is presented in Table 2 and includes the system used, the year, the category of the study and the target of the study. Finally, Figure 4 summarizes the main topics and characteristic of the systems used in the reviewed publications and shows the number of publications over the last 30 years that report the use of SCL in biomedical diffuse optics.

3.1. Novel Instrument Developement

The first paper reporting the use of a supercontinuum laser in biomedical diffuse optics was reported in the early nineties [29–31] by a group based at the Lund Laser Centre (LLC, Lund, Sweden). The femtosecond white light supercontinuum was generated by a Terawatt laser running at 10 Hz. The spectral decomposition was performed on the detection side, by coupling an imaging spectrometer and a streak camera, enabling to acquire parallelly the DTOF at all wavelengths. To improve the signal-to-noise ratio, the measurement had to be repeated for several laser shots, but the overall acquisition time was of just a few minutes, which is acceptable when no dynamic contrast is targeted. Using such a system, the very first in vivo absorption and scattering spectra of the female breast were acquired from 650 to 850 nm. This system was then updated in the early 2000s with a supercontinuum generation system based on a crystal fibre, which allowed to increase the optical power of the SCL generation [32].

Table 1. List of the SC laser-based systems used in the publications reviewed, with their principal characteristics. SC: SuperContinuum, FWHM: Full Widht at Half Maximum, CCD: Charge-Coupled Device, ICCD: Intensified Charge-Coupled Device, PMT: PhotoMultiplier Tube, SPAD: Single-Photon Avalanche Diode, SiPM: Silicon PhotoMultiplier, HPM: Hybrid Photodetector Module, sCMOS: scientific Complementary Metal–Oxide–Semiconductor, NIR: Near InfraRed.

System ID	Group	Year	SC Laser Type/Model	SC Laser System Characteristics				System Detection Characteristics	
				Spectral Capacity	Power (mW)	Repetition Rate (kHz)	Pulse Width (ps)	Detector Type	N° of Channels
1	Lund Institute of Technology, Lund, Sweden	1993	In-house	White light centred at 792 nm	1000	0.01	200	CCD camera	NA
2	Politecnico di Milano, Milan, Italy	2004	In-house	550–1100 nm	40	85,000	50–100	PMT	16
3	Lund Institute of Technology, Lund, Sweden	2004	In-house	500–1200 nm	NA	80,000	100	Streak camera	NA
4	Université Jean Monnet, Saint-Etienne, France.	2005	In-house	450–950 nm	1	1	170	Streak camera	NA
5	Politecnico di Milano, Milan, Italy	2006	In-house	550–1050 nm	100	NA	60–140	PMT	32
6	Politecnico di Milano, Milan, Italy	2007	SC450, Fianium	120 bands (600–1000 nm) FWHM = 5–20 nm	2600 (total)	20,000	10	SPAD	1
7	Lund University, Lund, Sweden	2009	SC500, Fianium	650–1400 nm	NA	80,000	50	PMT	2
8	Northeastern University, Boston, United States	2010	Koheras SuperK, NKT Photonics	550–850 nm	NA	80,000	30	PMT	16
9	National Optics Institute, Québec, Canada	2010	SC400, Fianium	Filtered at 660 nm	NA	40,000	90	PMT	1
10	Physikalisch-Technische Bundesanstalt, Berlin, Germany	2011	Fianium (model NA)	Tuned at 690 nm	NA	20,000	100	SPAD	1
11	University of California, Irvine, United States	2012	SC450, Fianium	680–850 nm	2000	20,000	3	PMT	2
12	Institute of Biocybernetics and Biomedical Engineering Polish Academy of Sciences, Warsaw, Poland	2012	SC450-4 (Fianium)	685–860, 16 bands	NA	40,000	NA	PMT	16
13	Politecnico di Milano, Milan, Italy	2012	SC450, Fianium	1100–1700 nm FWHM = 6.6–20.7 nm	6000 (total)	40,000	10	SPAD	1
14	Massachusetts General Hospital, Boston, United States	2013	SC600-8, Fianium	680, 710, 747, 760, 800, 820, 830, 840 nm	9000 (total)	60,000	NA	ICCD	175
15	Politecnico di Milano, Milan, Italy	2010	SuperK Extreme, NKT Photonics	600–1100 m	5000 (total)	2000–80,000	10	PMT	1

Table 1. *Cont.*

System ID	Group	Year	SC Laser Type/Model	SC Laser System Characteristics				System Detection Characteristics	
				Spectral Capacity	Power (mW)	Repetition Rate (kHz)	Pulse Width (ps)	Detector Type	N° of Channels
16	Katholieke Universiteit Leuven, Leuven, Belgium	2012	SC450-4, Fianium	450–2400 nm	4000 (total)	NA	NA	PINdiode	1
17	University College London, London, United Kingdom	2014	SC450, Fianium	690, 750, 800, 850 nm	4.5	40,000	4	PMT	32
18	Politecnico di Milano, Milan, Italy	2014	SC500-6, Fianium	Tuned at 800 nm	NA	40,500	NA	HPM	1
19	CREATIS, Université de Lyon, Lyon, France	2015	WhiteLase Micro, Fianium	500–1000 nm	10	2000	NA	ICCD	8
20	Politecnico di Milano, Milan, Italy	2015	SC450, Fianium	620 nm (40-nm bandwidth)	NA	80,000	NA	SPAD	1
21	Politecnico di Milano, Milan, Italy	2015	SC450, Fianium	750 nm (5-nm bandwidth)	NA	40,000	NA	SPAD	1
22	Politecnico di Milano, Milan, Italy	2015	SC450, Fianium	690 nm	NA	40,000	NA	SiPM	1
23	The City College of New York, New York, United States	2015	STM-2000-IR, Leukos	400–2500 nm	0.5/nm	NA	NA	IR-CCD	1
24	Politecnico di Milano, Milan, Italy	2015	SC450, Fianium	600–1350 nm	NA	40,000	NA	SiPM and PMT	2
25	Politecnico di Milano, Milan, Italy	2016	SC500-6, Fianium	760, 860 nm	30	40,500	NA	SPAD	1
26	Physikalisch-Technische Bundesanstalt, Berlin, Germany	2016	SC500-6, Fianium	Tuned at 650 nm	NA	40,500	100	SPAD	1
27	Politecnico di Milano, Milan, Italy	2017	Fianium (model NA)	750, 800, 850 nm	NA	40,000	NA	SPAD	2
28	State Key Laboratory of Precision Measuring Technology and Instruments, Tianjin University, Tianjin, China	2018	SC46 (YSL photonics)	1100–1350 nm (12 bands)	8000 (Total)	10–80,000	NA	InGaAs photodiode	1
29	Rensselaer Polytechnique Institute, Troy, United States	2018	MaiTai, Spectra Physics (1) SC Pro, YSL Photonics (2)	(1) 690–1040 nm FWHM = 15 nm (2) 400–2200 nm	(1) NA (2) 4000 (total)	(1) 80,000 (2) 25,000	(1) 100 (2) 150–200	PMT and NIR camera	2

Table 1. *Cont.*

System ID	Group	Year	SC Laser Type/Model	SC Laser System Characteristics				System Detection Characteristics	
				Spectral Capacity	Power (mW)	Repetition Rate (kHz)	Pulse Width (ps)	Detector Type	N° of Channels
30	Institute of Biocybernetics and Biomedical Engineering Polish Academy of Sciences, Warsaw, Poland	2018	SC450-4, Fianium	650–850 nm, 16 bands of 12.5 nm	NA	40,000–80,000	NA	PMT	1
31	University of Pennsylvania, Philadelphia, United States	2018	SuperK Extreme, NKT Photonics	730, 750, 786, 810, 830, 850 nm	NA	78,000	5	PMT	2
32	Physikalisch-Technische Bundesanstalt, Berlin, Germany	2019	FIU-15 PP, NKT Photonics	NA	NA	NA	NA	SPAD and HPM	2
33	University of Science and Technology, Trondheim, Norway	2019	SuperK Compact, NKT Photonics (1) SCT 500, Fyla (2)	NA	NA	20 (1) 20,000 (2)	NA	InGaAs detector	2
34	University of California, Irvine, United States	2019	SC400-2, Fianium	1000 bands (580–950 nm) FWHM = 17.25 nm (mean)	2000 (total)	NA	NA	sCMOS camera	NA
35	University College London, London, United Kingdom	2019	SC480-6, Fianium	16 bands (650–1100 nm) FWHM = 2–3 nm	6000 (total)	60,000	4	PMT	4
36	Physikalisch-Technische Bundesanstalt, Berlin, Germany	2019	SC500-6, Fianium	Tuned at 800 nm	NA	40,500	NA	HPM	1
37	Institute of Biocybernetics and Biomedical Engineering Polish Academy of Sciences, Warsaw, Poland	2020	FIU-15 PP, NKT Photonics	Tuned at 760 nm	NA	39,000	NA	HPM	1
38	University College London, London, United Kingdom	2021	WhiteLase Micro, Fianium	600, 630, 665, 784, 800, 818, 835, 851, 868, 881, 894 nm (FWHM = 6–11 nm)	0.06–0.11	NA	NA	sCMOS camera	NA
39	Biomedical Optics Research Laboratory, University Hospital Zurich and University of Zurich, Switzerland	2020	SuperK ExtremeEXR-15 (NKT)	Tuned at 800 nm	6000 (total)	80,000	NA	SPAD camera	NA

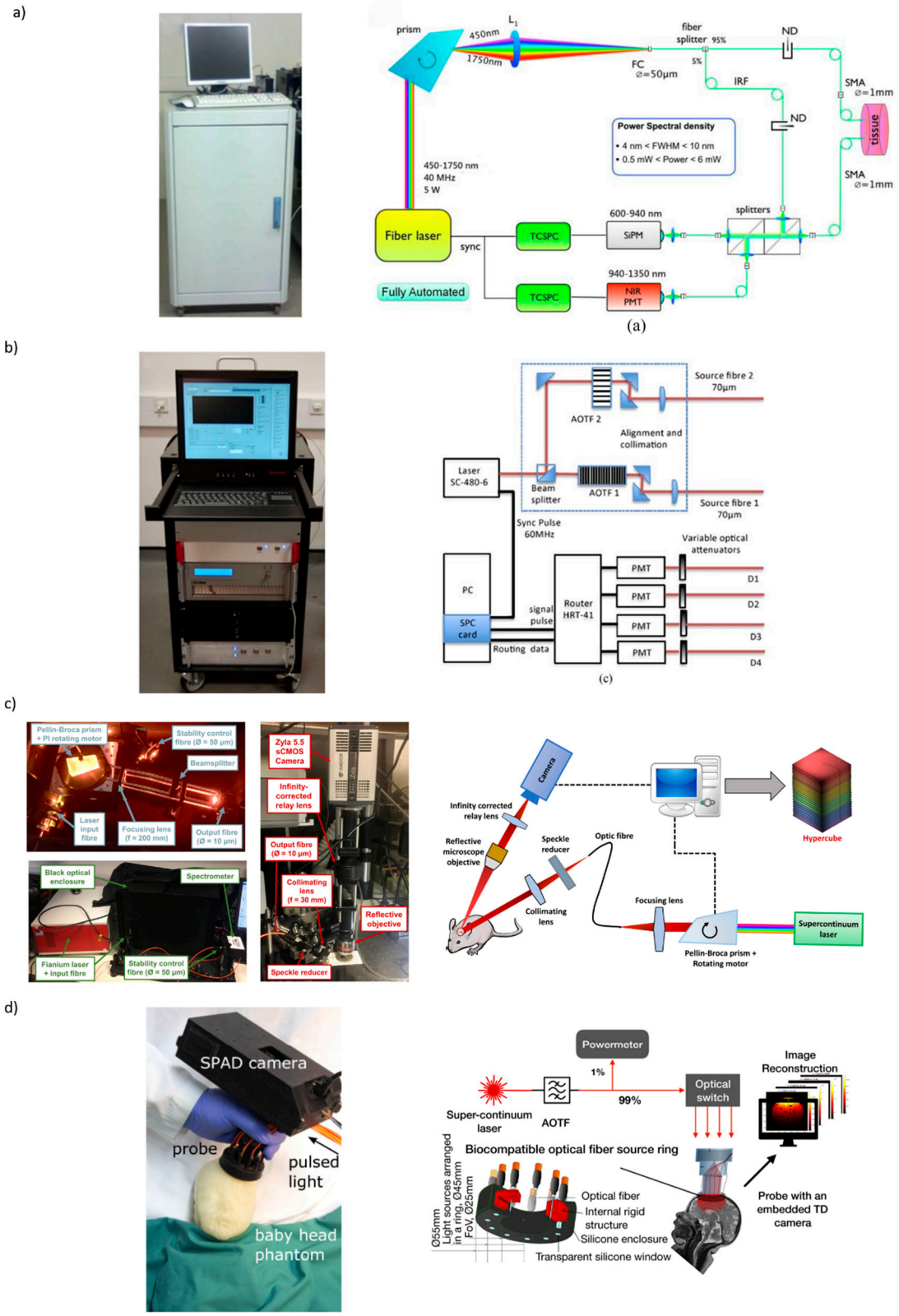

Figure 2. Pictures and schematic of various instruments based on SCL as a source. (**a**) TD-NIRS instrument aimed at broadband characterization of tissues. Figure reproduced from [23]. (**b**) TD-NIRS instrument aimed at monitoring both oxygenation and metabolism functional changes. Figure reproduced from [24]. (**c**) Preclinical instrument aimed at monitoring the exposed brain cortex of rodents. (reproduced with permission from [25], Copyright IEEE, 2021). (**d**) DOT system based on a SPAD camera aimed at functional brain monitoring in neonates. Figure reproduced from [26,27].

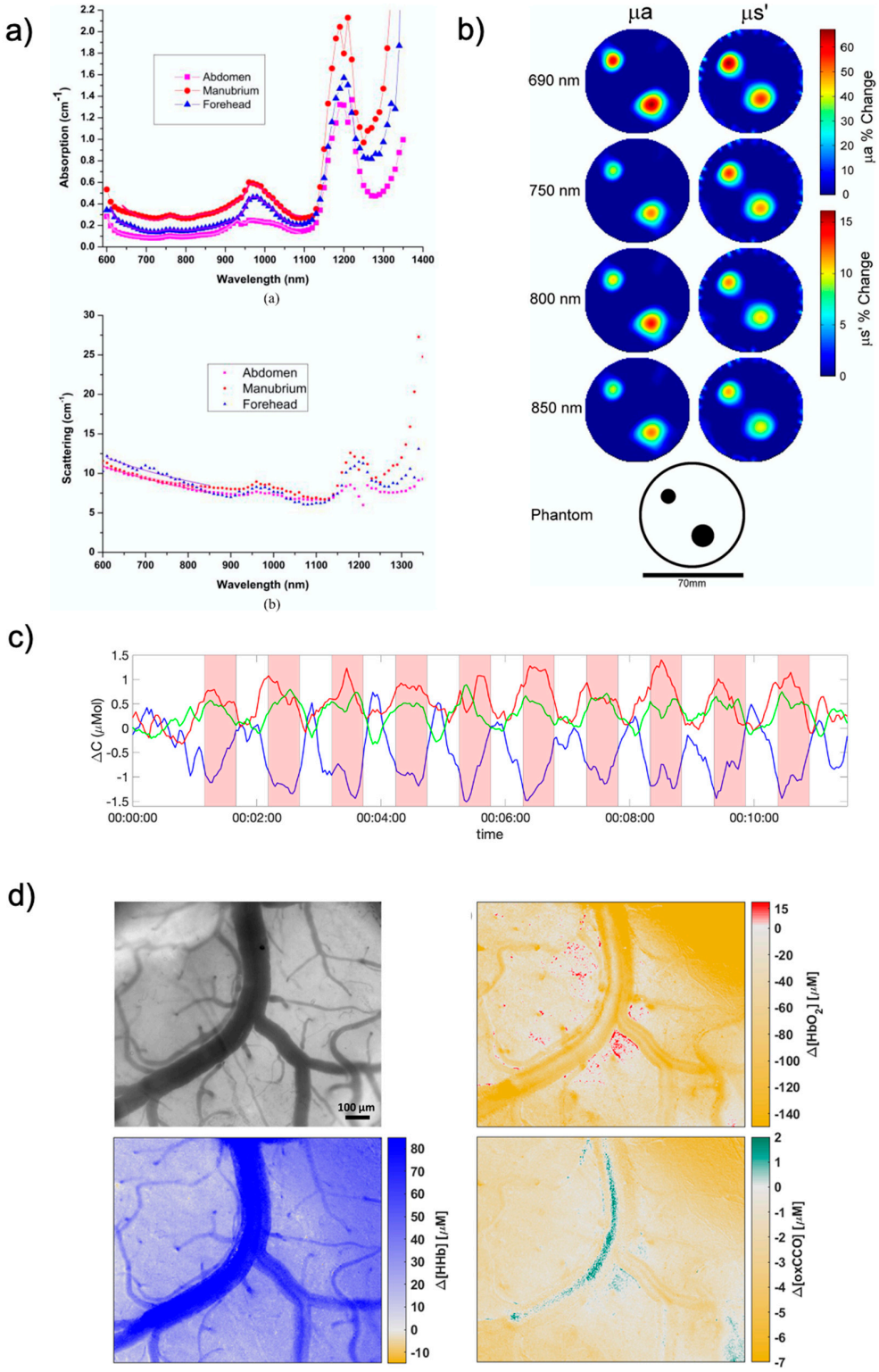

Figure 3. Example of typical data extracted form system based on SCL as sources. (**a**) absorption and reduce scattering coefficient of several tissues acquired the TD-NIRS system developed in ref [23]. Figure reproduced from [23]. (**b**) 2D maps of the changes in optical properties of a phantom using MONSTIR II. (reproduced with permission from [28], Copyright AIP Publishing, 2021). (**c**) Changes in [HbO2] (red), [HHb] (blue) and [oxCCO](green), in the occipital lobe, acquired with the MAESTROS system [24], during a typical brain activation. Data presented at the fNIRS conference in Tokyo in 2018. (**d**) Raw image and reconstructed variation in [HbO2], [HHb], and [oxCCO] acquired on the exposed cortex during anoxia. (reproduced with permission from [25], Copyright IEEE, 2021).

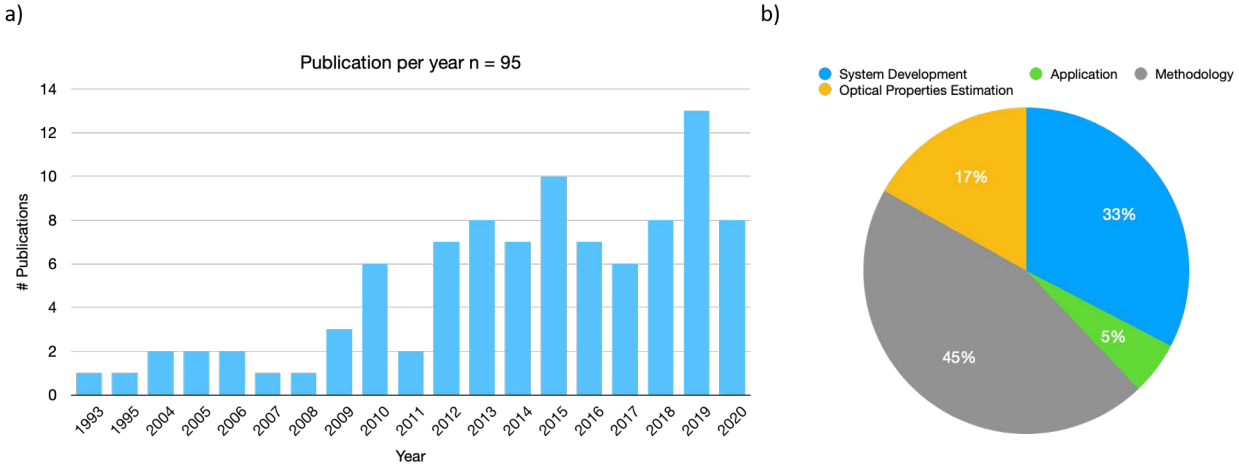

Figure 4. Summary of the literature review results. (**a**) Graph showing the number of publications using SCL in biomedical diffuse optics since the first study in 1993. (**b**) Summary of the main focus of the papers reviewed.

Parallel to these initial developments, a team based at Politecnico di Milano (POLIMI) produced a system able to characterise tissue between 610 and 1050 nm [33]. The system was however not based on a supercontinuum laser generation but on two tuneable lasers for the source, and the detection scheme was based on time-correlated single-photon counting (TCSPC), enabling light detection down to the single photon, which drastically improves the sensitivity of the system. This increased sensitivity is of great advantage to reduce the acquisition time and improve the light collection in the region where water absorption is high (900–1050). However, handling two lasers drastically increases the complexity and bulkiness of the system. Nevertheless, with that system, that team was able to record the optical properties of absorption and scattering of various tissues in-vivo [34–37]. The availability of commercial SCL sources gave rise to a new version of that system, where the 2 lasers were replaced by a SCL source coupled with a prism for the spectral selection [38]. This new source allowed to make the system more compact and transportable making it more suitable for the clinic. Moreover, the detector was also replaced (previously photomultiplier (PMT)) by a Single-Photon Avalanche Diode (SPAD) which enable to increase the spectral coverage, allowing a measurement between 600 and 1000 nm. This system could be used to characterise the optical and physiological properties of the tissue of the female breast. Another version of that system was developed, combining the SCL with a Ti-Sapphire laser to expand the spectral coverage to 1100 nm [39]. The SCL was used to cover the 600–900 nm and the Ti-Sapphire was used between 900 and 1100 nm. Indeed, even though the SCL could cover the entire considered wavelength band, the spectral resolution provided by the couple SCL/dispersion prism was too low to provide accurate results, as the source bandwidth increased with wavelength from 3 nm at 600 nm to 10 nm at 900 nm, and to approximately 15 nm at 1100 nm with that solution. This instrument has indeed been used to demonstrate that the broadening of the spectral bandwidth effect could impair the results, as the spectral region within the bandpass that exhibits the lowest absorption will dominate, leading to significant underestimations of the absorption and distortions in the spectral shape [40]. The spectral quality of the acquired data being extremely important, having the narrowest bandwidth is a great advantage. To do so, using a SCL is thus a true advantage as it provides a high power across the entire spectra. However, the method used to filter the white light is very important. As it has been seen above, several techniques can be used, either filtering on the detection side with a spectrometer, or on the source side with a dispersive prism or using an acousto-optic tuneable filter (AOTF), as we will see in systems described below. The POLIMI team has compared the wavelength selection from a SCL with an AOTF and a prism. They have

shown that one had to be careful when using AOTF, as they can produce side lobes in the selected bandpass, which can drastically impair the retrieval of the optical properties [41].

Nevertheless, the extension of the spectral coverage offered by this newly developed system was of particular interest, as several components, like lipid and collagen, have a distinct signature above 1000 nm. The LLC group also reported a similar system, based on a commercial SCL coupled with 2 AOTF and a detection scheme based on TCSPC with a coverage between 650 and 1400 nm [42]. The POLIMI group has then extended this work by focusing on the spectral window between 900 and 1700 nm, by using an InGaAs/InP SPAD as a detector [43–45]. Finally, they have produced a system able to cover the entire bandwidth from 600 to 1350 nm using a single SCL coupled with a prism for the wavelength selection, and 2 TCSPC cards couples with 2 detectors covering different bandwidth [23]. They managed to fix the issue of the spectral broadening induced by the prism by refining the optical chain. Additionally, this system was mounted on a 19-inch medical cart, making it easily used in a clinical environment. This system can be seen in Figure 2 and in an example of data in Figure 3. Moreover, by adjusting the detector used, the same instrument can be used to cover an even larger bandwidth, between 500 to 1700 nm [46].

With all these developments, POLIMI has been a major contributor to multispectral TD-NIRS and were able to characterize various tissue over a large bandwidth. They were able to characterize bones [47–49], thyroid tissues [50], adipose tissues [51], collagen [46,52], and elastin [53]. This groundwork was crucial in order to investigate the tissue composition of breast for example, which can help for diagnosis of cancerous tissue [54,55]. Finally, we can report that the latest reported system has also been used to monitor the thermal effect of Radio Frequency (RF) on tissues [56,57].

The previously reported systems were only composed of one channel, which can be a drawback when an image is required, like for performing mammography. Therefore, parallel to these developments, another system aimed at optical mammography was developed, based on a supercontinuum light generated in PCF and a 32-channel parallel detection [58]. This allowed to acquired image of the breast between 606 and 885 nm, and to extract hemoglobin, tissue saturation, lipid and water content, and scattering parameters of the tissue.

All the systems reported above were designed to collect spectral information about tissue, with a first application in breast cancer detection. Therefore, the acquisition time was not limited, and functional contrast was not explored. However, the potential of monitoring real time change in optical properties over a large bandwidth is quite appealing for various application, like brain monitoring [59]. Therefore, other systems were developed in order to achieve that goal. A system was developed at POLIMI based on a supercontinuum source generated in a PCF by a self-locking mode-locked Ti:Sapphire oscillator and a detection scheme based on an imaging spectrometer coupled to a 16-channel multianode PMT connected to a TCSPC board [60]. The fact that all the 16 wavelengths were captured at once enabled a fast acquisition and permitted to track dynamic variations in absorption and scattering spectra following hemodynamic changes [61]. The limitation of the detections scheme constraint the bandwidth of this system between 520 and 850 nm.

A similar approach was taken by a group based in Poland [62,63]. The system was based on a commercial SCL for the source, coupled to a 16-channel multianode PMT connected to a TCSPC board for the detection part. This system was used to follow a contrast agent (Indocyanine green (ICG)), which allows to estimate the cerebral blood perfusion. The same system can be used without ICG to monitor the intrinsic optical contrast [64]. Similarly, the author and colleagues used a TD-NIRS system based on a SCL filtered at 808 nm and on a detection scheme based on a single channel TCSPC to follow ICG bolus [65]. The novelty of this study was the fact that the TD-NIRS was coupled with a diffuse correlation spectroscopy system (DCS) [66]. The coupling of these two techniques allowed to retrieve absolute cerebral blood flow measurement in patients in the intensive care unit, showing that these systems could be used in a particularly difficult clinical

environment. Moreover, the possibility to also measure blood perfusion is of great interest and might help in the adoption of the technique in the clinic.

Another potential detection scheme in order to collect parallel data is to use an Intensified CCD (ICCD) camera. Selb and collaborators used a commercial SCL combined with a ICCD camera to perform functional brain imaging with 2 wavelengths at a frequency of 3 Hz [67]. This system was an upgrade of a previously developed instrument based on pulsed Ti:Sapphire laser [68]. This source was tuneable but the switching time between wavelength was too slow to enable dual-wavelength functional imaging. Therefore, the authors report that the use of SCL unlocked this possibility with their detection scheme.

Similarly, Lange and collaborators described a TD-NIRS system developed to measure the human brain tissue physiology [69,70]. This system was based on commercial SCL for the emission and on an ICCD camera coupled with an imaging spectrometer in order to perform the spectral decomposition. This system allowed to retrieve the typical hemodynamic response, and preliminary results on the detection of oxCCO were also performed. The ability to retrieve oxCCO is exiting for brain applications, as it has been shown that this contrast can be more specific than the oxygenation, and that it can be an early biomarker of neonatal encephalopathy for example [7]. This possibility has been explored by the UCL team by developing a 4-channel 16 wavelengths TD-NIRS system in order to monitor both the oxygenation and oxCCO signal [24,71]. This system was based on time multiplexing, with a TCSPC detection scheme, but the fast-switching capabilities of the SCL coupled with AOTF allowed the acquisition of all the 16 wavelengths in less than 2 s. This system has also been used to evaluate the long-term reproducibility of the evaluation of cerebral tissue saturation in healthy adults with good reproducibility [72]. This system can be seen in Figure 2, and in an example of data in Figure 3.

Another approach that has been used using SCL sources is the development of non-contact systems. This can present several advantages to avoid issues attributed to sensor-tissue contact like skin compression and to obtain a reduction in measurement preparation time. A team at the Physikalisch-Technische Bundesanstalt (PTB) has developed a non-contact TD-NIRS system based on a commercial SCL and fast-gated SPAD to explore the human brain physiology [73–76]. At the time, the authors reported that the use of SCL permitted a shorter pulse width (<100 ps), an achievable output power considerably larger than picosecond diode lasers, and the possibility to quickly switch between two different wavelengths (i.e., on the µs to ms time scale). Moreover, the use of the SPAD in that system enables to reject the burst of early photons, which can improve the spatial resolution of the system at very short detector distances [77]. This process had been previously demonstrated by the POLIMI team that had develop a single channel TD-NIRS system based on SCL and a fast gated SPAD detector [78]. The POLIMI team has also worked on the modelling of the parameters of such detection schemes, in order to optimise their design [79].

The non-contact scheme is also very useful for pre-clinical applications. Indeed, several systems, based on SCL for the source, aiming at collecting physiological information of small animals, have been proposed. In the early 2000s, a system based on a home-made SC generation associated with an imaging spectrometer coupled with a streak camera was developed and used to monitor the cerebral hemodynamic of songbirds [80,81]. More recently, the UCL team have developed a system aiming at investigating both the cerebral hemodynamic and metabolic response (via oxCCO) of the exposed cortex of rodents [25]. In this work, a commercial SCL was used in combination with a dispersive prism, for the emission, and a sCMOS camera, as a detector, to record 11 images (11 wavelengths) of the exposed cortex in less than 0.3 s/wavelength. Here the recording was not time resolved, but the power of the laser and the ability to quickly switch between the wavelength had dictated the choice of this source. This system can be seen in Figure 2 and an example of data in Figure 3. Another approach can be to use spatial frequency domain imaging (SFDI), a wide-field, noncontact, model-based technique that can quantitatively assess absorption and scattering, on a pixel-by-pixel basis by calculating the modulation transfer function

of structured light projected onto the tissue. This technique can be hyperspectral if a proper source is used. However, the system developed thus far was based on conventional broadband sources coupled with tunable filters, which limited their acquisition speed and spectral resolution. Torabzadeh and colleagues [82] applied this technique using the principles of the single-pixel compressive sensing. They used a commercial SCL coupled with a dispersive prism to achieve a final bandwidth 1000 spectral bands between 580 and 950 nm, which was larger than the previously developed systems. With this system, the authors were able to characterize the optical properties of a beef sample ex-vivo in 2D, and extract physiological information (i.e., hemoglobin content and fat and water content). The authors noted that the wavelength selection technique used was still slow (i.e., 150 s of acquisition time for a 4 cm × 6 cm), but that switching to an AOTF solution could greatly improve this speed. Using the same principle of the single-pixel compressive sensing, Farina and colleagues reported a TD-DOT instrument based on time-resolved single pixel camera [83]. Their approach was based on a SCL source filtered at 620 nm coupled with a digital micromirror device (DMD) to generate the spatial pattern. The time domain acquisition was based on TCSPC. Pian and colleagues used a similar approach but expended it to a broadband illumination and detection [84]. The authors reported that their system, aimed at fluorescence molecular tomography, benefitted for the commercial SCL source to perform hyperspectral excitation of the sample which offers a spectral information boost within the same data acquisition time compared to single wavelength excitation situations.

Another work aiming at improving the spatial resolution of TD-DOT was to investigate the effect of only considering early photons, which undergo fewer scattering events [85]. In this work, this approach has been tested using a commercial SCL together with a bandpass filter at 670 nm. It worth noting that the commercial version of this laser was modified by the manufacturer so that it had a shortened fibre compared to standard models, which reduced the pulse width to approximately 300 ps. This is important as the benefit of the gating of the early photons is highly dependent on the instrument response function (IRF) of the system. The authors reported that with this technique, and this instrument, a 64 to 84% image resolution could be achieved, which could be a great benefit for preclinical imaging with diffuse optics.

Novel algorithms can also be used in combination to TD-DOT instruments to recovers 3D images of the optical properties and physiological parameters. A team in Grenoble has explored the use of the Mellin-Laplace transform to reconstruct 3D images of the chromophores inside phantoms and for the non-invasive assessment of flap viability in rats' models. There instrumentation was based on commercial SCL, coupled with either an AOTF or an interferential filter, for the source and a TCPSC scheme for the detection [86,87].

TD-DOT has also been explored in humans, in order to reconstruct 2D or 3D maps of the optical properties and hemodynamic parameters. To this end, the UCL team had design MONSTIR II to perform tomographic brain imaging [28]. This system is based on a commercial SCL with an AOTF filtering and has 32 channels based on TCSPC. It was successfully used to scan healthy and ill infants in a clinical environment [88,89], an example of data produced by this system is provided in Figure 3. More recently, a new TD-DOT system based on a commercial SCL filtered by an AOTF, and a 32 × 32-pixel SPAD camera, has been developed by a team at the Biomedical Optics Research Laboratory at the University of Zurich [26,27,90]. This system operates at 2 wavelengths and at 11 sources points, which can be scanned in about 3 s. It is a big step forward compared to previously developed system, especially considering its size, as it is handheld. A picture of this instrument is reported in Figure 2.

Finally, all the instrument mentioned above were mostly based on the TD technique, or traditional white light illumination. We can note that we found one frequency domain (FD) system, that is based a commercial SCL to collect our system collects FD data at 170 wavelengths from 680 to 850 nm and allows to accurately measure absorption and scattering information about the tissue [91].

3.2. Methodology

We have seen that the SCL has been used to develop several systems, mainly aiming at characterising the optical properties of tissues over a large bandwidth or to non-invasively follow the oxygenation and/or metabolic changes both in humans and in preclinical models. Both of these capacities are extremely appealing for clinical applications. However, the transition to the clinical application of system based on SCL and more generally TD-NIRS/DOT is still happening at a slow pace. One of the reasons of the slow adoption of optical techniques is the lack of standards in the community. Indeed, standardisation is key in order to test all the systems on the same ground, and reenforce the trustworthiness of the technique. In the recent years, standardisation have been a main goal of the NIRS community, and several protocols have been developed in order to compare and test the capabilities of NIRS systems. The main produced protocols were the MEDPHOT [92], BIP [93], and nEUROpt [94]. It is out of the scope of this paper to describe these protocols in detail, but the cornerstones of all of these are to produce standard phantoms, well characterized spectrally in terms of absorption and scattering coefficients, in order to be able to quantitatively compare different systems or methods. In this matter, SCL based systems were extensively used to characterize the material used to produce these phantoms and the actual final phantoms used as standard. These optical phantoms can either be solid (easier to store and stable over a long period of time) or liquid (easier to precisely tune the optical properties of the solution and to adjust it dynamically). For the liquid phantoms, the core principle is to use a fatty solution to control the scattering coefficient of the solution, and ink to control their absorption properties. Several recipes have been tested, like using Agar and Triton [95], but the most common recipe to date is to use a combination of water, intralipid and Indian ink. This choice has arisen after a careful characterization of both intralipid and Indian ink, principally with instrument based on SCL [96–100]. We can note that for the precise optical characterisation of liquid, techniques based on integrating sphere are often used. However, this methodology cannot be applied for large solid phantoms. In this matter, TD-NIRS has proved a good methodology to accurately estimates the optical properties. For example, in 2010, Bouchard and colleagues used a TD-NIRS setup based on a SCL source filtered at 610 nm in order to estimate the optical properties of phantom with an absolute error estimates of 0.01 cm^{-1} (11.3%) and 0.67 cm^{-1} (6.8%) for the absorption coefficient and reduced scattering coefficient, respectively [101].

On top of designing phantom able to mimic the background optical properties of tissues, some methods have emerged to mimic a perturbation of the absorption coefficient within a homogeneous medium. To that end, one can either use a liquid phantom for the homogeneous medium, and a small black PVC target for the perturbation. A protocol has been designed and it is possible to precisely set the absorption perturbation value based on the size of the black PVC inclusion [94]. This protocol has been validated with Monte Carlo simulations and in-situ using a system based on SCL [102]. A similar phantom based on a completely solid phantom, with a movable solid rod, has also been designed and characterised [103]. Lastly, some phantoms have also been characterized in order to be a tool to evaluate quantitatively the responsivity of NIRS systems [104].

Finally, we can also mention new approaches based on digital phantoms. Basically, rather than physically simulating the process of light propagation in tissue, the digital phantom provides the detector with light signals mimicking the signals obtained in-vivo. Such systems based on an integrating sphere and several light sources, including a commercial SCL, have been proposed to spectrally characterise and calibration optical systems [105]. More recently, a digital phantom has been developed to mimic TD-NIRS signal acquisition, and the authors used various sources and detectors in order to test this approach, including a SCL [106]. One other important component to optically characterize is the optode holders used to secure the optical fibres to the patient. In a recent study, Amendola and colleagues used a system previously developed to evaluate the optical properties of fruit [107] (based on a commercial SCL and a filter wheel to select 14 spectral band in the range 550 to 940 nm) to spectrally characterised poly lactic acid (PLA), a material used for

3D printing [108]. As 3D printing is more and more common in order to produce probe holders, it is important to optically characterise the material used in order to avoid any unwanted effects on the measurement provoked by light interaction with the material. In that study, the authors concluded that the different material tested were not optically the same, and that characterisation was important before their use.

The development of all these phantoms has provided a good framework for the developers to compare their systems and methods in order to provide robust clinical information. Regarding the instrumentation, a lot of effort are currently being made in order to improve the detection scheme of TD-NIRS. To that end, SCL have been a source of choice to test new detectors like the promising fast silicon photomultiplier (SiPM) which drastically improve light harvesting compared to the old PMTs [109–111]. SCL based systems have also been used to characterise novel bio-compatible fibres that can be implanted in the patient with potential use in the monitoring of the evolution of the physiology after a surgical intervention or in photodynamic therapy (PDT) [112,113].

Regarding the methodology, several new data processing techniques have been explored and tested in conjunction with SCL. Indeed, system based on SCL can collect multidimensional data that can be coupled together in order to improve the accuracy of the data, reduce the noise or explore new contrast. One of the first work regarding this matter dates from 2006, where D'Andrea and colleagues, showed that one could increase the robustness of the determination of the chromophore's concentrations in tissues (hemoglobin, water, lipid) by using a spectral constraint during the fitting procedure [114]. This showed the strength of using the spectral dimension coupled with the DTOF, which is accessible when using SCL. This method has also been used to monitor absorption changes in a layered diffusive medium [115], which is relevant in the monitoring of brain activation for example. Similar approaches were explored in the same group in order to accurately monitor the spectral changes in absorption coefficients of turbid media [116].

One can also use the spatial dimension in order to enhance the amount of information recorded, by recording data from multiple source-detector distances. This approach has been recently tested and it has been shown that coupling the spatial dimension with the DTOF could increase the accuracy of the estimation of the optical properties [117–119]. Another interesting use of the spatial dimension is the self-calibrating method for TD-NIRS, which uses the spatial dimension in order to avoid the measurement of the IRF, that is needed to remove the effect of the instrument from the response of the tissue [120]. The characterisation of the IRF necessitates an extra step that can be a burden in a clinical environment. Therefore, this method could facilitate the use of TD-NIRS in the clinic. Finally, we can also report that an approach combining the spatial and spectral dimension proved to also improve the accuracy of the results of CW-NIRS. This has been tested recently, especially with blood phantoms and compared to the results of a TD-NIRS instrument based on a SCL source [121].

The large amount of data collected by TD-NIRS also enables different data processing scheme to extract the relevant information. Therefore, there is a need to properly compare all the available methods in order to evaluate their strength and weaknesses. This work has recently been undertaken in order to compare the moment and time windowing techniques [122,123]. Having a deep understanding of all the data processing method is also crucial so the proper technique can be used depending on the application.

Several multi-centre initiatives have recently promoted this standardisation effort to compare instruments and algorithms. To that end, partners from the BitMap network (http://www.bitmap-itn.eu/, accessed date: 1 February 2021) have started comparing instruments from different institutions all over Europe, by using the same sets of solid phantoms from the 3 main protocols [124,125]. Moreover, several centres in Europe have used their instruments (several based on SCL) on 9 subjects, to study the inter-subject variability of the optical properties of the human head measured by several instruments [126]. They could show that the inter-subject variability was significant, with a big effect of the technique used (either CW or TD) because of their different depth sensitivity, which in

turn affects the averaged optical properties retrieved. Therefore, it is evident that all the efforts to precisely characterized instruments and methods will have a huge impact on the precision of the optical measurement of tissue parameters.

Finally, the use of SCL can help to explore new avenues in diffuse optics. The main one is to go above the "therapeutical window" in the second (1100 nm to 1350 nm) and the third (1600 to 1870 nm) near-infrared optical window. On top of the previously reported works that expand the bandwidth of TD-NIRS systems up to 1700 nm, Sordillo and colleagues reported the use of a commercial SCL source, filtered with a bandpass and long pass filters to target the second and third NIR windows, coupled with an IR-CCD camera, to acquire transmission images of 3 targets embedded in chicken tissue of various thickness [127]. They were able to distinguish the targets up to a depth of 10 mm, which was not possible when using the same setup but with a traditional lamp source. These results are promising in order to implement transmission measurement, especially for preclinical imaging.

As we have seen previously, the use of these long NIR wavelength is useful to resolve more chromophores like collagen. It is also promising to resolve glucose, which could be a true benefit for several clinical applications like monitoring diabetes [128], or monitoring brain injuries [129] or neonatal encephalopathy [130]. Once again, in this wavelength range, the power delivered by SCL has proved efficient to monitor the glucose contrast in the NIR [131,132].

Finally, a tentative to non-invasively probe the lungs with a TD-NIRS system based on SCL source was reported [133]. The measurements were performed on three subjects, and spectra from 600 to 1100 nm could be acquired. Here, the depth sensitivity of a TD-NIRS is essential and this application shows that instruments based on that technology could be used to non-invasively probes tissues previously thought out of reach.

Table 2. Table of the literature review of the use of SC lasers in biomedical diffuse optics. The system used in each study are described more in detail in Table 1 and referred to as "system ID". μ_a: absorption coefficient, μ'_s: reduced scattering coefficient.

Publication	Year	System ID	Category of Study	Target of Study	Reported Quantities
S. Andersson-Engels et al. [29]	1993	1	System development	Multispectral tissue characterisation	μ_a
af Klinteberg et al. [30]	1995	1	Optical properties estimation	Breast tissue examination	μ_a, μ'_s
Bassi et al. [60]	2004	2	System development	Phantoms and in vivo validation measurements	μ_a, μ'_s
Abrahamsson et al. [32]	2004	3	System development	Sample characterisation	μ_a, μ'_s
Swartling et al. [61]	2005	3	System development	Phantoms and in vivo validation measurements	μ_a, μ'_s, [HbT], StO_2
Ramstein et al. [81]	2005	4	System development	Optical properties in vivo monitoring of songbird brain	μ_a, μ'_s
D'Andrea et al. [114]	2006	2	Methodology	Validation of spectral fitting analysis	μ_a, μ'_s, H_2O, Water Content Lipid Content, [HbO_2], [HHb], [HbT], StO_2
Bassi et al. [58]	2006	2	System development	Optical mammography	μ_a, μ'_s, H_2O, Lipid Content, [HbT], StO_2
Bassi et al. [38]	2007	6	System development	Phantoms and in vivo breast validation	μ_a, μ'_s, H_2O, Lipid Content, [HbO_2], [HHb], [HbT], StO_2
Vignal et al. [134]	2008	4	Application	In vivo measurement of brain hemodynamic changes in songbird	[HbO_2], [HHb], [HbT]
Farina et al. [40]	2009	6	Methodology	Study and correction of bandpass effects in TD spectroscopy	μ_a
Taroni et al. [39]	2009	6	System development	In vivo measurements of breast tissue	μ_a, μ'_s, Water Content, Lipid Content, Collagen Content, [HbT], StO_2
Svensson et al. [42]	2009	7	System development	Validation on phantoms	μ_a, μ'_s
Valim et al. [85]	2010	8	Methodology	Study of PDSF in phantoms	Photon density sensitivity function (PDSF)
Bouchard et al. [101]	2010	9	Methodology	Characterisation of tissue-mimicking phantoms	n, g, μ_a, μ'_s
Pifferi et al. [116]	2010	15	Methodology	Data processing	$\Delta\mu_a$
Taroni et al. [52]	2010	15	Optical properties estimation	Characterisation of collagen optical properties	μ_a, μ'_s
Giusto et al. [115]	2010	2	Methodology	Data Processing	μ_a, μ'_s, [HbO_2], [HHb]
Dalla Mora et al. [78]	2010	6	Methodology	Electronic development	μ_a, μ'_s
Mottin et al. [80]	2011	4	Application	In vivo study of brain oxygen uncoupling/recoupling in songbirds	[HbO_2], [HHb]
Mazurenka et al. [73]	2011	10	System development	Non-contact TD-NIRS	Contrast
Arnesano et al. [91]	2012	11	System development	FD spectroscopy for tissue imaging	μ_a, μ'_s
Spinelli et al. [97]	2012	Multiple systems	Optical properties estimation	Characterisation of liquid phantoms	Intrinsic absorption coefficient, Intrinsic reduced scattering coefficient
Bargigia et al. [44]	2012	13	System development	Characterisation on lipids	μ_a, μ'_s
Gerega et al. [63]	2012	12	Methodology	TD-NIRS with ICG	Fluorescence of ICG
Bargigia et al. [43]	2012	15	System development	Bandwidth up to 1700 nm	μ_a, μ'_s

Table 2. *Cont.*

Publication	Year	System ID	Category of Study	Target of Study	Reported Quantities
Xu et al. [105]	2012	Laser not specified	Methodology	Digital phantom	StO_2
Wang et al. [96]	2012	16	System development	Liquid optical phantom characterisation in the second and third optical window	g, μ_a, $\mu´_s$
Selb et al. [67]	2013	14	System development	Functional brain imaging	$\Delta[HbO_2]$, Δ[HHb]
Bargigia et al. [45]	2013	13	System development	In vivo measurements of forearm and breast	Water Content, Lipid Content, Collagen Content
Farina et al. [41]	2013	6	Methodology	Comparison of approaches for spectral selection	μ_a, $\mu´_s$
Mazurenka et al. [75]	2013	26	System development	Non-contact system	$\Delta[HbO_2]$, Δ[HHb]
Wabnitz et al. [135]	2013	Multiple instruments	Methodology	multi-laboratory study to assess the performance of time-domain optical brain imagers	μ_a, $\mu´_s$
Quarto et al. [95]	2013	15	Methodology	Phantom characterisation	μ_a, $\mu´_s$
Aernouts et al. [98]	2013	16	Optical properties estimation	Phantom characterisation	g, μ_a, $\mu´_s$
Quarto et al. [133]	2013	15	Methodology	In vivo optical diagnostics of lung conditions and diseases	μ_a, $\mu´_s$
Aernouts et al. [99]	2014	16	Optical properties estimation	Phantom characterisation	g, μ_a, $\mu´_s$
Spinelli et al. [100]	2014	6	Optical properties estimation	Phantom characterisation	μ_a, $\mu´_s$
Cooper et al. [28]	2014	17	System development	Brain TD-DOT	μ_a, $\mu´_s$
Farina et al. [126]	2014	Multiple instruments	Optical properties estimation	Brain Tissue characterisation	μ_a, $\mu´_s$
Wabnitz et al. [93]	2014	17	Methodology	Instrumental performance protocol	Instrument parameters
Wabnitz et al. [94]	2014	17	Methodology	Instrumental performance protocol	Instrument parameters, μ_a
Martelli et al. [102]	2014	18	Methodology	Phantom characterization	μ_a, $\mu´_s$
Taroni et al. [55]	2015	6	Optical properties estimation	In vivo quantification of collagen in breast tissue	Water Content, Lipid Content, Collagen Content, Collagen index, [HbT], StO_2
Lange et al. [70]	2015	19	System development	Functional brain monitoring	$\Delta[HbO_2]$, Δ[HHb], Δ[oxCCO]
Farina et al. [83]	2015	20	System development	TD-DOT/FMT	Fluorescence
Contini et al. [79]	2015	21	Methodology	Time-gated measurements on tissue phantoms	Contrast
Della Mora et al. [109]	2015	22	Methodology	Testing of a SiPM	μ_a, $\mu´_s$
Pifferi et al. [103]	2015	15	Methodology	Phantom characterisation	μ_a, $\mu´_s$
Martinenghi et al. [110]	2015	15	Methodology	Characterisation of SiPM detectors	Instrument parameters
Dempsey et al. [88]	2015	17	Methodology	Whole-head TD-DOT in neonates	μ_a, $\mu´_s$
Sordillo et al. [127]	2015	23	Methodology	Deep-tissue, optical properties monitoring	μ_t

Table 2. *Cont.*

Publication	Year	System ID	Category of Study	Target of Study	Reported Quantities
Konugolu Venkata Sekar et al. [47]	2015	24	Optical properties estimation	In vivo measurement of optical properties of bone	μ_a, μ'_s, Water Content, Lipid Content, Collagen Content, [HbO_2], [HHb], [HbT], StO_2
Konugolu Venkata Sekar et al. [23]	2016	24	Optical properties estimation	In vivo human tissues measurements	μ_a, μ'_s, H_2O, Lipid, Collagen, [HbO_2], [HHb], [HbT], StO_2
Di Sieno et al. [76]	2016	25	System development	Validation on phantoms	Instrument parameters
Wabnitz et al. [104]	2016	26	Optical properties estimation	Phantoms characterisation	μ_a, μ'_s
Konugolu Venkata Sekar et al. [49]	2016	24	Optical properties estimation	In vivo measurement of optical properties of bone	μ_a, μ'_s, Water Content, Lipid Content, Collagen Content, [HbO_2], [HHb], StO_2
Konugolu Venkata Sekar et al. [48]	2016	24	Optical properties estimation	In vivo measurement of optical properties of bone	μ_a, μ'_s, Water Content, Lipid Content, Collagen Content, [HbO_2], [HHb], [HbT], StO_2
Martinenghi et al. [111]	2016	13	Methodology	Characterisation of SiPM detectors	Instrument parameters
Di Sieno et al. [87]	2016	27	System development	In vivo assessment of flap viability	[HbO_2], [HHb]
Zouaoui et al. [86]	2017	22	Methodology	Validation of chromophore decomposition algorithm	Dyes content
Konugolu Venkata Sekar et al. [46]	2017	24	Optical properties estimation	In vivo measurement of optical properties of collagen	μ_a Collagen
Wabnitz et al.[74]	2017	27	Methodology	Non-contact TD brain imaging	Intensity Contrast
Di Sieno et al. [112]	2017	24	Methodology	Characterisation of bioresorbable fibres	μ_a, μ'_s
Konugolu Venkata Sekar et al. [53]	2017	24	Optical properties estimation	In vivo measurement of optical properties of elastin	μ_a and μ'_s Elastin
Jiang et al. [90]	2017	39	Methodology	Data Processing—GPU	μ_a, μ'_s
Konugolu Venkata Sekar et al. [50]	2018	24	Optical properties estimation	In vivo chromophore characterisation of thyroid	μ_a, μ'_s
Lange et al. [69]	2018	19	System development	In vivo monitoring of brain physiological changes in humans	Δ[HbO_2], Δ[HHb]
Pian et al. [84]	2018	29	System development	Validation on phantoms	μ_a
Gerega et al. [62]	2018	30	Application	assessment of intracerebral and extracerebral absorption changes	Δ[ICG]
He et al. [65]	2018	31	Application	continuous monitoring of absolute cerebral blood flow (CBF) in adult human patients	CBF
Della Mora et al. [113]	2018	15	Methodology	bioresorbable optical fibers	Contrast, μ_a, μ'_s
Laura Dempsey [89]	2018	17	System development	Brain TD-DOT	[HbO_2], [HHb]
Liu et al. [131]	2018	28	Methodology	Glucose monitoring	[Glucose]
Wabnitz et al. [106]	2019	32	Methodology	Validation of digital phantom	Phantom parameters and basic responses of the instrument to it

Table 2. *Cont.*

Publication	Year	System ID	Category of Study	Target of Study	Reported Quantities
Fuglerud et al. [132]	2019	33	Methodology	Glucose sensing in blood	[Glucose]
Torabzadeh et al. [82]	2019	34	System development	Spatial FD HIS on ex vivo beef sample	μ_a, μ'_s, Water Content, lipid Content, [HbO_2], [HHb], [MHb]
Lange et al. [24]	2019	35	System development	Validation on phantoms	μ_a, μ'_s, [HbO_2], [HHb], [oxCCO]
Ferocino et al. [54]	2019	24	Methodology	Validation on phantoms of TD-NIRs reconstruction algorithm	μ_a, μ'_s
Lange et al. [72]	2019	35	Application	Reproducibility analysis of cerebral oxygenation measured with TD-NIRS	[HbO_2], [HHb], StO_2
Yang et al. [118]	2019	36	Methodology	Validation on phantoms of a multivariate TD-SD algorithm	μ_a, μ'_s
Yang et al. [117]	2019	36	Methodology	Validation on phantoms of a multivariate TD-SD algorithm	μ_a, μ'_s
Ferocino et al. [136]	2019	24	Methodology	Validation on meat samples of TD-NIRs reconstruction algorithm	[HbO_2]
Wojtkiewicz et al. [120]	2019	30	Methodology	Validation on phantoms and in vivo of a self-calibrating TD algorithm	μ_a, μ'_s, [HbO_2], [HHb]
Sudakou et al. [64]	2019	30	System development	Multi wavelength TD-NIRS system for brain monitoring	[HbO_2], [HHb], [HbT]
Wabnitz et al. [122]	2020	17	Methodology	Depth-selective analysis in TD optical brain imaging	μ_a, μ'_s
Lanka et al. [51]	2020	24	Optical properties estimation	In vivo measurement of optical properties of adipose tissue	μ_a, μ'_s, Water Content, Lipid Content, Collagen Content, [HbO_2], [HHb], [HbT], StO_2
Sudakou et al. [123]	2020	37	Methodology	Performance of measurands in TD optical brain imaging	μ_a, μ'_s
Yang et al. [119]	2020	32	Methodology	Space-enhanced TD diffuse optics in two-layered structures	μ_a, μ'_s
Lanka et al. [56]	2020	24	Methodology	Monitoring of thermal treatment in biological tissues	μ_a, μ'_s
Amendola et al. [108]	2020	24	Methodology	Effect of the 3d printed material on raw data	Photon Counts
Jiang et al. [26]	2020	39	System development	Novel TD-NIRS system based on SPAD camera	μ_a, μ'_s
Jiang et al. [27]	2020	39	Methodology	Image reconstruction for TD-NIRS system based on SPAD system	μ_a
Kovacsova et al. [121]	2021	35	Methodology	Validation of broadband oximetry algorithm	μ_a, μ'_s, StO_2
Giannoni et al. [25]	2021	38	System development	HSI of in vivo hemoglobin and CCO in the exposed cortex of mice	Δ[HbO_2], Δ[HHb], Δ[oxCCO]

4. Discussion

We have summarized the use of SCL sources in biomedical diffuse optics. Historically, these sources were allowed to develop TD-NIRS system as they could deliver a pulsed coherent light at several MHz with narrow pulse width in order to reduce the IRF [137], and high power, of several mW/Wavelength, which were characteristically difficult to achieve in the early 1990s. Moreover, the development of commercially available compact SCL in the 2000s also helped the development of the use of these sources, and we have reported that more companies (see Figure 1) are now able to provide such sources.

The main advantage of these sources is that they make it easier to explore more wavelength, enabling a multispectral or even broadband or hyperspectral measurement. Several measurement strategies can be implemented in order to do so. The first one is to use the white light as a source and achieve the spectral unmixing at the detection stage. The first available option to do so was to use an imaging spectrometer coupled with a streak camera, which achieve very high temporal resolution (in terms of arrival time of photons). However, this solution was bulky, and the sensitivity of these camera was low compared to the newest detection technologies. The same method can be used by either coupling the spectrometer with an ICCD camera, or a 16-channel TCSPC. This approach of performing the spectral unmixing on the detection can achieve faster measurement since no spectral switching mechanism is employed. However, the resolution of these approaches, either spectrally or temporally, can be limited. For example, typical ICCD cameras have a gate width of 200 ps, which limits the temporal resolution of the DTOF. On the other end, the 16-channel TCSPC system used by Sudakou and colleagues [64] allows spectral bands of 12.5 nm, limiting the spectral resolution. The other option to perform the spectral unmixing is to do a sequential acquisition, by filtering the white light on the source side. To do so, two main approach are used, (1) using an AOTF, with the ability of fast switching (few microseconds) but with a potential degradation of the spectral response (i.e., side lobs), and (2), using a dispersing prism which can be mounted on a rotating axis, which can achieve better spectral performances but at the cost of a slower switching time. Therefore, the choice of the instrumentation depends on the end application, and trade-off needs to be made between spectral quality and acquisition speed. Whatever the requirement, we have seen that SCL can be used and coupled with various type of instrumentation in order to accommodate to the requirements of the applications.

From an application point of view, the ability to monitor a large number of several wavelengths has several advantages. First of all, it enables to provides a true spectroscopic analysis, both in terms of absorption and scattering. This is extremely appealing for cancer application, where this type of "optical biopsy", enables to distinguish between healthy and cancerous tissue. This type of application has been extensively used in breast cancer [138,139], and more recently, thyroid applications [50,140]. In this type of application, where the spectral quality is the most important criteria, the second instrumental approach, based on spectral unmixing with a dispersing prism, was used. Secondly, the first instrumental approach, based on spectral unmixing at the detection stage, or the second instrumental approach using ATOF, give the possibility to acquire several wavelengths, either parallelly, or with a fast switching, in a time scale compatible with functional imaging. With these approaches, several authors have explicitly noted that the adoption of SCL enabled them to design or update existing systems, in order to retrieve dynamic physiological information [67,75].

The large number of wavelengths enabled by SCL also give the possibility to go beyond the traditional contrasts, like the hemodynamic one, in order to get information about metabolism for example, by extracting information about more chromophores, like oxCCO [7,24]. We can also note that beyond the intrinsic optical signal, a contrast agent, like ICG, can also be used in order to get information on tissue perfusion. This has notably been extensively used to monitor cerebral perfusion, and the SCL has also proved to be a suitable light source for these applications, even used in extremely complicated clinical settings like ICUs [65].

From a historical point of view, we can note that the development of commercial fibre also largely helped with the adoption of that technology. Indeed, out of the 35 different systems used in the reviewed paper, only 4 (less than 12%) are home-made. They correspond to the system developed before 2010. Past that date, all systems reviewed used a commercial source. We can also see the increase number of papers since the adoption of the commercial sources, with a number of papers published per year roughly doubling from that date. One of the main advantages reported by the authors when they adopted commercial SCL was their relative compactness, compared to the initial development of SC generation. This can be seen in Figure 2, with systems able to be mounted on trolley compatible with the clinical environment. However, the use of these lasers in actual clinical studies remains marginal. In our recent review [141], which has explored the use of TD-NIRS for clinical applications, less than 4% of the 52 papers reviewed were using a system based on a SCL source. Indeed, despite their advantages, a few drawbacks still hindered the adoption of SCL as a standard source. The first one is the cost which, despite a significant decrease in the recent years, remains high (i.e., more than 20,000 pounds for a SCL with several watts of power, enabling a final power of at least 1 mW per wavelength). The second main disadvantage is the warmup time, and the overall stability of these sources. Indeed, the stability of the output can be a concern, but the use of a reference arm can solve this issue [23]. This of course comes at the cost of a more complicated and bulkier instrument. Regarding the warmup time, typically, 1 h is required so the instrument reach thermal equilibrium, which can be too long for certain clinical applications. Some recent TD-NIRS systems based on pulsed laser diode have reported a warmup time of only 15 min, which is way more advantageous in a clinical setting [142]. Finally, even though the novel commercial SCL are more compact than in the early days, their size is still significantly bigger than traditional pulsed laser diode, which limit the reduction of the overall instrument size. Therefore, this can also slow down the adoption of these systems, as space are often very limited in busy clinical environment like ICUs.

These drawbacks are less of an issue for the preclinical settings as the environment is way less constrained. Therefore, the great potential of applications based on SCL outweighs its current main drawbacks, and several instruments based on SCL have been developed for preclinical imaging. The interested reader can refer to the recent review by Bérubé-Lauzière and colleagues, which explore more particularly the use of DOT in preclinical settings [143]. It worth noting that these systems are non-contact, and that this particular detection approach has also been explored for human imaging. Here, having an extremely narrow pulse, like the one provided by SCL, is of great interest as one can take advantage of the null-source approach [77]. Even if these approaches are less common, they can have potential great applications for perioperative measurements, or when the patient is difficult to access, and represent a promising avenue.

The above-mentioned drawbacks are also less problematic in a typical lab setting. SCL are a great tool for teams aiming at instrumental and methodological developments. In the reviewed papers, 33% were aimed at the initial system developments, and 18% and 44% were focused on optical tissue estimations or methodological developments, respectively. Only 5% of the reported studies were focused on pure applications, like tissue oxygenation estimation or cancer monitoring. Indeed, the availability of these SCL sources in teams focused on methodological and instrumental developments have pushed their used to test new possibilities and enhance the reliability of the system by promoting standardization. It is worth mentioning that having a SCL is not mandatory in a lot of settings, and that these sources were used as they were available in most of the groups working on instrumental and methodological developments. Indeed, in the case of a CW system, we have seen that SCL systems were used to provide a high number of wavelengths. In that case, other broadband sources are available, like Tungsten Halogen Light Sources (THLS) or like the Laser-Driven Light Sources (LDLS). The main disadvantage of the THLS is the low power density/wavelength, compared to coherent sources, which can limit their possibilities in biomedical diffuse optics. However, we can still report that THLS were successfully used

to developed simple CW instruments [144,145]. On the contrary, the novel LDLS are of interest as they can produce a stable, high power broadband light. This technology is still relatively new and, to our knowledge, has not been used in biomedical diffuse optics yet. However, its attractive characteristics could be of interest for developing CW biomedical diffuse optics systems. The interested reader can refer to review [146] for more details. Finally, we can note that designing a multi-wavelengths CW system by adding up several single wavelengths light sources, like LEDs, is possible, but it is limited to a low number of wavelengths as the bulkiness and cost of the systems would rapidly increase with the number of wavelengths. In the case of TD systems, the choice of the light source is also largely dictated by the number of wavelengths needed, as can be seen in Table 3, that summarizes the relative advantages and disadvantages of single wavelength laser diode sources versus SCL in two cases: (1) low and (2) high number of wavelengths for TD systems. The use of single wavelength laser diode sources is indeed well adapted when a low number of wavelengths is required, as these sources are compact and relatively not expensive regarding the SCL ones. However, if one wants to design a truly spectroscopic system, with a high number of wavelengths required, these advantages became less evident as, similarly to the CW case, the bulkiness and cost of the system increase as function as the number of wavelengths. This is even more pronounced for the TD cases as the electronics are more complex. Finally, we can mention that if one wants to focus on methodological development, when specific wavelengths are still not defined, the flexibility of SCL is then evident as this choice does not have to be made from the start of the designing process, and not all the wavelengths are available commercially with laser diodes. Therefore, even though other light sources with characteristics compatible with diffuse optics are available, the high power, broadband spectrum, and fast switching capabilities of SCL makes them a source of choice, sufficiently versatile to be able to explore various avenues without source limitations.

Table 3. Main relative advantages and drawbacks of single wavelength laser diode sources and SCL as function as the number of wavelengths used for TD systems. (+ advantages / − disadvantages). FW: Few Wavelength, HNW: High number of Wavelengths.

	Single Wavelength Sources		**Supercontinuum Laser**	
	Few Wavelengths	High number of Wavelengths	Few Wavelengths	High Number of Wavelengths
Cost	++	−−	−−	+
Stability	+	+	−	−
Compactness	++	−−	−−	+
Wavelength Choice	Limited	Limited	Unlimited	Unlimited
Overall	+++	−−	−−	++

This spectral flexibility offered by SCL has indeed been a true advantage regarding the standardization efforts, giving the ability to optically characterize over a large bandwidth material and tissue. Phantom materials, like Intralipid or Indian ink, have been able to be precisely characterized using SCL, enabling to produce reproducible recipes for liquid phantoms, or to produces reliable solid phantoms. This now gives the possibility to accurately and quantitatively test and compare newly developed instruments and algorithms. We can note the effort undertaken by the BitMap project that have started comparing instruments, from different institutions all over Europe, using the same sets of solid phantoms [124,125].

SCL can also be used as companions to develop new electronical components. Indeed, one of the big instrumental development in the recent year have been the refinement of the detection scheme. Especially, a lot of improvement have been seen in novel solid state detectors [147] which enable to boost light harvesting detectors electronics. The development of gated detector [148] also enables techniques like null source distance to be practically implemented, which can improve the resolution and sensitivity of the

technique [77]. In these works, the availability of SCL sources enabled to perform a precise characterisation of these detectors in situ, both in terms of temporal resolution, thanks to the short pulse width of the SCL, and in terms of spectral responsivity over a large bandwidth. The combination of the SCL capabilities with these new detectors can notably boost the capabilities of TD-NIR instrument, overcoming some current limitations like, for example, the penetration depth [22,149].

The inherent ability of SCL sources to construct systems gathering multidimensional information, i.e., spatial/spectral/temporal, also makes them a perfect tool to test novel algorithms able to exploit this large amount of data. The recent works by Yang and colleagues [117–119] show the advantages of using multi-dimensional datasets, by enhancing the accuracy of the optical properties estimation of tissues by using simultaneously the temporal and spatial dimensions. Kovacsova and colleagues [121] also showed this utility, here combining the spectral and the spatial dimensions. It worth noting that this work is based on broadband CW-NIRS, but that the results of this algorithm has been tested against a TD-NIRS instrument based on SCL as a source. Combining all the dimensions available is certainly a really exiting avenue for the field of diffuse optics, to make the system even more robust and precise.

Finally, we can mention that in the recent years, progress has also been made in individual pulsed laser source, which now achieve several 10th of mW and a pulse width shorter than 100 ps. A good example of the uses of these sources can be found in [150], where an 8 wavelengths TD-NIRS system, compatible for breast imaging for example, has been developed. This paves the way on the use of these sources to enable miniaturisation of TD-NIRS instruments, making them truly compatible with the clinic. These sources could then replace the SCL in clinical settings. However, depending on the application and the chromophores targeted, the wavelength selection is a process that requires some investigations in order to balance the system complexity, and the possible crosstalk effects between the chosen wavelengths. Therefore, systems based on SCL able to easily explore various combinations of wavelengths are once more extremely useful. Lastly, the flexibility of these systems also allows to explore new horizons and applications area, like we have seen with exploring contrast above the classical therapeutic windows (i.e., above 1000 nm) [46], or to explore new organs, like lungs [133]. Therefore, even though the main drawbacks of SCL in terms of absolute cost, size, and stability might prevent their use on a wide scale in the clinical world, their main advantages in terms of power, wavelength choice, and relatively low cost for high number of wavelengths is likely to still push their use in the labs to drive forward the clinical innovation in biomedical diffuse optics.

5. Conclusions

We have seen that the use of SCL drove the developments in biomedical diffuse optics, and particularly in TD-NIRS. First of all, it is a tool of choice to estimate the optical properties of tissues and phantom material over a large bandwidth. This knowledge is crucial in order to develop a standardized method, and to provide a-priori information used in the calculation of in vivo chromophores concentration for example. Moreover, the high spectral power combined with the ability to easily and quickly select wavelength make SCL suitable not only for in vivo tissue characterization, and application like breast cancer monitoring, but also to follow fast dynamic physiological processes like cerebral hemodynamic. The large number of wavelength available in the systems based on SCL (several systems reported parallel or quasi-parallel acquisition of up to 16 wavelengths) not only enables to refine the precision of the measurement, but also provides extra information about different processes like metabolism. These sources are also relevant to design instrument aiming at non-contact scanning, which make them also a good candidate for preclinical applications. In conclusion, SCL are a valuable tool at every step of the developmental and translational work, from fundamental characterization to preclinical and clinical use, and we have no doubt that it will still be an important brick to keep driving the innovation in biomedical diffuse optics.

Author Contributions: F.L., L.G. and I.T. conceived and designed the study. F.L. conducted the literature search and drafted the first version of the paper. L.G. created Tables 1 and 2. All authors have read and agreed to the published version of the manuscript.

Funding: This research was funded by the Medical Research Council (MR/S003134/1).

Institutional Review Board Statement: Not applicable.

Informed Consent Statement: Not applicable.

Conflicts of Interest: The authors declare no conflict of interest. The funders had no role in the design of the study; in the collection, analyses, or interpretation of data; in the writing of the manuscript, or in the decision to publish the results.

References

1. Elwell, C.E.; Cooper, C.E. Making light work: Illuminating the future of biomedical optics. *Philos. Trans. R. Soc. A Math. Phys. Eng. Sci.* **2011**, *369*, 4358–4379. [CrossRef] [PubMed]
2. Maniewsk, R.; Liebert, A.; Kacprzak, M.; Zbieć, A. Selected applications of near infrared optical methods in medical diagnosis. *OptoElectron. Rev.* **2004**, *12*, 255–262.
3. Martelli, F.; Binzoni, T.; Pifferi, A.; Spinelli, L.; Farina, A.; Torricelli, A. There's plenty of light at the bottom: Statistics of photon penetration depth in random media. *Sci. Rep.* **2016**, *6*, 27057. [CrossRef] [PubMed]
4. Wolf, M.; Ferrari, M.; Quaresima, V. Progress of near-infrared spectroscopy and topography for brain and muscle clinical applications. *J. Biomed. Opt.* **2007**, *12*, 62104.
5. Scholkmann, F.; Kleiser, S.; Metz, A.J.; Zimmermann, R.; Mata Pavia, J.; Wolf, U.; Wolf, M. A review on continuous wave functional near-infrared spectroscopy and imaging instrumentation and methodology. *Neuroimage* **2014**, *85*, 6–27. [CrossRef] [PubMed]
6. Yeganeh, H.Z.; Toronov, V.; Elliott, J.T.; Diop, M.; Lee, T.-Y.; St Lawrence, K. Broadband continuous-wave technique to measure baseline values and changes in the tissue chromophore concentrations. *Biomed. Opt. Express* **2012**, *3*, 2761–2770. [CrossRef] [PubMed]
7. Bale, G.; Elwell, C.E.; Tachtsidis, I. From Jöbsis to the present day: A review of clinical near-infrared spectroscopy measurements of cerebral cytochrome-c-oxidase. *J. Biomed. Opt.* **2016**, *21*, 091307. [CrossRef]
8. Yamada, Y.; Suzuki, H.; Yamashita, Y. Time-Domain Near-Infrared Spectroscopy and Imaging: A Review. *Appl. Sci.* **2019**, *9*, 1127. [CrossRef]
9. Grosenick, D.; Wabnitz, H.; Macdonald, R. Diffuse near-infrared imaging of tissue with picosecond time resolution. *Biomed. Eng. Biomed. Tech.* **2018**, *63*, 511–518. [CrossRef] [PubMed]
10. Torricelli, A.; Contini, D.; Pifferi, A.; Caffini, M.; Re, R.; Zucchelli, L.; Spinelli, L. Time domain functional NIRS imaging for human brain mapping. *Neuroimage* **2014**, *85*, 28–50. [CrossRef]
11. Konugolu Venkata Sekar, S.; Lanka, P.; Farina, A.; Dalla Mora, A.; Andersson-Engels, S.; Taroni, P.; Pifferi, A. Broadband Time Domain Diffuse Optical Reflectance Spectroscopy: A Review of Systems, Methods, and Applications. *Appl. Sci.* **2019**, *9*, 5465. [CrossRef]
12. Hoshi, Y.; Yamada, Y. Overview of diffuse optical tomography and its clinical applications. *J. Biomed. Opt.* **2016**, *21*, 091312. [CrossRef]
13. Durduran, T.; Choe, R.; Baker, W.B.; Yodh, A.G. Diffuse optics for tissue monitoring and tomography. *Rep. Prog. Phys.* **2010**, *73*, 076701. [CrossRef]
14. Labruyère, A.; Tonello, A.; Couderc, V.; Huss, G.; Leproux, P. Compact supercontinuum sources and their biomedical applications. *Opt. Fiber Technol.* **2012**, *18*, 375–378. [CrossRef]
15. Alfano, R.R.; Shapiro, S.L. Emission in the Region 4000 to 7000 A Via Four-Photon Coupling in Glass. *Phys. Rev. Lett.* **1970**, *24*, 584–587. [CrossRef]
16. Alfano, R.R.; Shapiro, S.L. Observation of Self-Phase Modulation and Small-Scale Filaments in Crystals and Glasses. *Phys. Rev. Lett.* **1970**, *24*, 592–594. [CrossRef]
17. Granzow, N. Supercontinuum white light lasers: A review on technology and applications. In Proceedings of the Joint TC1—TC2 International Symposium on Photonics and Education in Measurement Science, Jena, Germany, 17–19 September 2019; Volume 11144, p. 1114408.
18. Bloembergen, N. Nonlinear optics: Past, present, and future. *IEEE J. Sel. Top. Quantum Electron.* **2000**, *6*, 876–880. [CrossRef]
19. Agrawal, G.P. Nonlinear fiber optics: Its history and recent progress [Invited]. *J. Opt. Soc. Am. B* **2011**, *28*, A1–A10. [CrossRef]
20. Knight, J.C.; Birks, T.A.; Russell, P.S.J.; Atkin, D.M. All-silica single-mode optical fiber with photonic crystal cladding. *Opt. Lett.* **1996**, *21*, 1547–1549. [CrossRef] [PubMed]
21. Tu, H.; Boppart, S.A. Coherent fiber supercontinuum for biophotonics. *Laser Photonics Rev.* **2013**, *7*, 628–645. [CrossRef]
22. Pifferi, A.; Contini, D.; Mora, A.D.; Farina, A.; Spinelli, L.; Torricelli, A. New frontiers in time-domain diffuse optics, a review. *J. Biomed. Opt.* **2016**, *21*, 091310. [CrossRef] [PubMed]

23. Konugolu Venkata Sekar, S.; Dalla Mora, A.; Bargigia, I.; Martinenghi, E.; Lindner, C.; Farzam, P.; Pagliazzi, M.; Durduran, T.; Taroni, P.; Pifferi, A.; et al. Broadband (600–1350 nm) Time-Resolved Diffuse Optical Spectrometer for Clinical Use. *IEEE J. Sel. Top. Quantum Electron.* **2016**, *22*, 406–414. [CrossRef]
24. Lange, F.; Dunne, L.; Hale, L.; Tachtsidis, I. MAESTROS: A Multiwavelength Time-Domain NIRS System to Monitor Changes in Oxygenation and Oxidation State of Cytochrome-C-Oxidase. *IEEE J. Sel. Top. Quantum Electron.* **2018**, *25*. [CrossRef] [PubMed]
25. Giannoni, L.; Lange, F.; Sajic, M.; Smith, K.J.; Tachtsidis, I. A hyperspectral imaging system for mapping haemoglobin and cytochrome-c-oxidase concentration changes in the exposed cerebral cortex. *IEEE J. Sel. Top. Quantum Electron.* **2021**, *27*. [CrossRef] [PubMed]
26. Jiang, J.; Mata, A.D.C.; Lindner, S.; Charbon, E.; Wolf, M.; Kalyanov, A. Dynamic time domain near-infrared optical tomography based on a SPAD camera. *Biomed. Opt. Express* **2020**, *11*, 5470. [CrossRef]
27. Jiang, J.; Mata, A.D.C.; Lindner, S.; Zhang, C.; Charbon, E.; Wolf, M.; Kalyanov, A. Image reconstruction for novel time domain near infrared optical tomography: Towards clinical applications. *Biomed. Opt. Express* **2020**, *11*, 4723. [CrossRef] [PubMed]
28. Cooper, R.J.; Magee, E.; Everdell, N.; Magazov, S.; Varela, M.; Airantzis, D.; Gibson, A.P.; Hebden, J.C. MONSTIR II: A 32-channel, multispectral, time-resolved optical tomography system for neonatal brain imaging. *Rev. Sci. Instrum.* **2014**, *85*. [CrossRef] [PubMed]
29. Andersson-Engels, S.; Berg, R.; Persson, A.; Svanberg, S. Multispectral tissue characterization with time-resolved detection of diffusely scattered white light. *Opt. Lett.* **1993**, *18*, 1697. [CrossRef]
30. af Klinteberg, C.; Berg, R.; Lindquist, C.; Andersson-Engels, S.; Svanberg, S. Diffusely scattered femtosecond white-light examination of breast tissue in vitro and in vivo. *Photon Propag. Tissues* **1995**, *2626*, 149–157.
31. Jarlman, O.; Berg, R.; Andersson-Engels, S.; Svanberg, S.; Pettersson, H. Time-resolved white light transillumination for optical imaging. *Acta Radiol.* **1997**, *38*, 185–189. [CrossRef]
32. Abrahamsson, C.; Svensson, T.; Svanberg, S.; Andersson-Engels, S.; Johansson, J.; Folestad, S. Time and wavelength resolved spectroscopy of turbid media using light continuum generated in a crystal fiber. *Opt. Express* **2004**, *12*, 4103–4112. [CrossRef]
33. Pifferi, A.; Torricelli, A.; Taroni, P.; Comelli, D.; Bassi, A.; Cubeddu, R. Fully automated time domain spectrometer for the absorption and scattering characterization of diffusive media. *Rev. Sci. Instrum.* **2007**, *78*, 053103. [CrossRef] [PubMed]
34. Taroni, P.; Pifferi, A.; Torricelli, A.; Comelli, D.; Cubeddu, R. In vivo absorption and scattering spectroscopy of biological tissues. *Photochem. Photobiol. Sci.* **2003**, *2*, 124–129. [CrossRef]
35. Pifferi, A.; Torricelli, A.; Taroni, P.; Bassi, A.; Chikoidze, E.; Giambattistelli, E.; Cubeddu, R. Optical biopsy of bone tissue: A step toward the diagnosis of bone pathologies. *J. Biomed. Opt.* **2004**, *9*, 474. [CrossRef] [PubMed]
36. Cubeddu, R.; Pifferi, A.; Taroni, P.; Torricelli, A.; Valentini, G. Noninvasive absorption and scattering spectroscopy of bulk diffusive media: An application to the optical characterization of human breast. *Appl. Phys. Lett.* **1999**, *74*, 874–876. [CrossRef]
37. Taroni, P.; Pifferi, A.; Cubeddu, R.; Torricelli, A.; Comelli, D. Absorption of collagen: Effects on the estimate of breast composition and related diagnostic implications. *J. Biomed. Opt.* **2007**, *12*, 014021. [CrossRef]
38. Bassi, A.; Farina, A.; D'Andrea, C.; Pifferi, A.; Valentini, G.; Cubeddu, R. Portable, large-bandwidth time-resolved system for diffuse optical spectroscopy. *Opt. Express* **2007**, *15*, 14482. [CrossRef]
39. Taroni, P.; Bassi, A.; Comelli, D.; Farina, A.; Cubeddu, R.; Pifferi, A. Diffuse optical spectroscopy of breast tissue extended to 1100 nm. *J. Biomed. Opt.* **2009**, *14*, 054030. [CrossRef] [PubMed]
40. Farina, A.; Bassi, A.; Pifferi, A.; Taroni, P.; Comelli, D.; Spinelli, L.; Cubeddu, R. Bandpass Effects in Time-Resolved Diffuse Spectroscopy. *Appl. Spectrosc.* **2009**, *63*, 48–56. [CrossRef]
41. Farina, A.; Bargigia, I.; Taroni, P.; Pifferi, A. Note: Comparison between a prism-based and an acousto-optic tunable filter-based spectrometer for diffusive media. *Rev. Sci. Instrum.* **2013**, *84*. [CrossRef]
42. Svensson, T.; Alerstam, E.; Khoptyar, D.; Johansson, J.; Folestad, S.; Andersson-Engels, S. Near-infrared photon time-of-flight spectroscopy of turbid materials up to 1400 nm. *Rev. Sci. Instrum.* **2009**, *80*, 45–48. [CrossRef]
43. Bargigia, I.; Tosi, A.; Farina, A.; Bassi, A.; Taroni, P.; Bahgat Shehata, A.; Della Frera, A.; Dalla Mora, A.; Zappa, F.; Cubeddu, R.; et al. Optical Spectroscopy up to 1700 nm: A Time-Resolved Approach Combined with an InGaAs/InP Single-Photon Avalanche Diode. In Proceedings of the Biomedical Optics and 3-D Imaging 2012, Miami, FL, USA, 28 April–2 May 2012; p. JM3A.16.
44. Bargigia, I.; Tosi, A.; Bahgat Shehata, A.; Della Frera, A.; Farina, A.; Bassi, A.; Taroni, P.; Dalla Mora, A.; Zappa, F.; Cubeddu, R.; et al. Time-resolved diffuse optical spectroscopy up to 1700 nm by means of a time-gated InGaAs/InP single-photon avalanche diode. *Appl. Spectrosc.* **2012**, *66*, 944–950. [CrossRef]
45. Bargigia, I.; Tosi, A.; Bahgat Shehata, A.; Della Frera, A.; Farina, A.; Bassi, A.; Taroni, P.; Dalla Mora, A.; Zappa, F.; Cubeddu, R.; et al. In-vivo optical spectroscopy in the time-domain beyond 1100 nm. In Proceedings of the Optics InfoBase Conference Papers, Munich, Germany, 12–16 May 2013; Taroni, P., Dehghani, H., Eds.; Optical Society of America: Washington, DC, USA, 2013; p. 879902.
46. Sekar, S.K.V.; Bargigia, I.; Mora, A.D.; Taroni, P.; Ruggeri, A.; Tosi, A.; Pifferi, A.; Farina, A. Diffuse optical characterization of collagen absorption from 500 to 1700 nm. *J. Biomed. Opt.* **2017**, *22*, 015006. [CrossRef] [PubMed]
47. Konugolu Venkata Sekar, S.; Farina, A.; Martinenghi, E.; Dalla Mora, A.; Taroni, P.; Pifferi, A.; Negredo, E.; Puig, J.; Escrig, R.; Rosales, Q.; et al. Time-resolved diffused optical characterization of key tissue constituents of human bony prominence locations. In Proceedings of the European Conference on Biomedical Optics, Munich, Germany, 21–25 June 2015; Volume 9538, pp. 95380X–95380X–5.

48. Konugolu Venkata Sekar, S.; Pagliazzi, M.; Negredo, E.; Martelli, F.; Farina, A.; Dalla Mora, A.; Lindner, C.; Farzam, P.; Pérez-Álvarez, N.; Puig, J.; et al. In Vivo, non-invasive characterization of human bone by hybrid broadband (600–1200 nm) diffuse optical and correlation spectroscopies. *PLoS ONE* **2016**, *11*, e0168426. [CrossRef]
49. Sekar, S.K.V.; Mora, A.D.; Martinenghi, E.; Taroni, P.; Pifferi, A.; Farina, A.; Puig, J.; Negredo, E.; Lindner, C.; Pagliazzi, M.; et al. In vivo Time domain Broadband (600–1200 nm) Diffuse Optical Characterization of Human Bone. In Proceedings of the Optical Tomography and Spectroscopy 2016, Fort Lauderdale, FL, USA, 25–28 April 2016; p. JTu3A.32.
50. Konugolu Venkata Sekar, S.; Farina, A.; Dalla Mora, A.; Lindner, C.; Pagliazzi, M.; Mora, M.; Aranda, G.; Dehghani, H.; Durduran, T.; Taroni, P.; et al. Broadband (550–1350 nm) diffuse optical characterization of thyroid chromophores. *Sci. Rep.* **2018**, *8*, 1–8. [CrossRef]
51. Lanka, P.; Segala, A.; Farina, A.; Konugolu Venkata Sekar, S.; Nisoli, E.; Valerio, A.; Taroni, P.; Cubeddu, R.; Pifferi, A. Non-invasive investigation of adipose tissue by time domain diffuse optical spectroscopy. *Biomed. Opt. Express* **2020**, *11*, 2779. [CrossRef] [PubMed]
52. Taroni, P.; Bassi, A.; Farina, A.; Cubeddu, R.; Pifferi, A. Role of Collagen Scattering for in vivo Tissue Characterization. In Proceedings of the Biomedical Optics 2010, Miami, FL, USA, 11–14 April 2010; p. BTuD107.
53. Konugolu Venkata Sekar, S.; Beh, J.S.; Farina, A.; Dalla Mora, A.; Pifferi, A.; Taroni, P. Broadband diffuse optical characterization of elastin for biomedical applications. *Biophys. Chem.* **2017**, *229*, 130–134. [CrossRef] [PubMed]
54. Ferocino, E.; Di Sciacca, G.; Di Sieno, L.; Dalla Mora, A.; Pifferi, A.; Arridge, S.R.; Martelli, F.; Taroni, P.; Farina, A. Multi-wavelength time domain diffuse optical tomography for breast cancer: Initial results on silicone phantoms. In Proceedings of the SPIE BiOS, San Francisco, CA, USA, 2–7 February 2019; p. 59.
55. Taroni, P.; Pifferi, A.; Quarto, G.; Farina, A.; Ieva, F.; Paganoni, A.M.; Abbate, F.; Cassano, E.; Cubeddu, R. Time domain diffuse optical spectroscopy: In vivo quantification of collagen in breast tissue. In Proceedings of the Optical Methods for Inspection, Characterization, and Imaging of Biomaterials II, Munich, Germany, 21–25 June 2015; Volume 9529, p. 952910.
56. Lanka, P.; Joseph, F.K.; Kruit, H.; Konugolu, S.; Sekar, V.; Farina, A.; Cubeddu, R.; Manohar, S.; Pifferi, A. Time domain diffuse optical spectroscopy for the monitoring of thermal treatment in biological tissue. In Proceedings of the Optical Tomography and Spectroscopy 2020, Washington, DC, USA, 20–23 April 2020; pp. 1–2.
57. Kalloor Joseph, F.; Lanka, P.; Kruit, H.; Konugolu Venkata Sekar, S.; Farina, A.; Cubeddu, R.; Manohar, S.; Pifferi, A. Key features in the optical properties of tissue during and after radiofrequency ablation. In Proceedings of the SPIE BiOS, San Francisco, CA, USA, 1–6 February 2020; p. 16.
58. Bassi, A.; Spinelli, L.; D'Andrea, C.; Giusto, A.; Swartling, J.; Pifferi, A.; Torricelli, A.; Cubeddu, R. Feasibility of white-light time-resolved optical mammography. *J. Biomed. Opt.* **2006**, *11*, 054035. [CrossRef]
59. Ferrari, M.; Mottola, L.; Quaresima, V. Principles, techniques, and limitations of near infrared spectroscopy. *Can. J. Appl. Physiol.* **2004**, *29*, 463–487. [CrossRef]
60. Bassi, A.; Swartling, J.; D'Andrea, C.; Pifferi, A.; Torricelli, A.; Cubeddu, R. Time-resolved spectrophotometer for turbid media based on supercontinuum generation in a photonic crystal fiber. *Opt. Lett.* **2004**, *29*, 2405. [CrossRef]
61. Swartling, J.; Bassi, A.; D'Andrea, C.; Pifferi, A.; Torricelli, A.; Cubeddu, R. Dynamic time-resolved diffuse spectroscopy based on supercontinuum light pulses. *Appl. Opt.* **2005**, *44*, 4684. [CrossRef] [PubMed]
62. Gerega, A.; Milej, D.; Weigl, W.; Kacprzak, M.; Liebert, A. Multiwavelength time-resolved near-infrared spectroscopy of the adult head: Assessment of intracerebral and extracerebral absorption changes. *Biomed. Opt. Express* **2018**, *9*, 2974. [CrossRef]
63. Gerega, A.; Milej, D.; Weigl, W.; Zolek, N.; Sawosz, P.; Maniewski, R.; Liebert, A. Multi-wavelength time-resolved measurements of diffuse reflectance: Phantom study with dynamic inflow of ICG. In Proceedings of the Biomedical Optics 2012, Miami, FL, USA, 28 April–2 May 2012; p. JM3A.31.
64. Sudakou, A.; Lange, F.; Isler, H.; Gerega, A.; Ostojic, D.; Sawosz, P.; Tachtsidis, I.; Wolf, M.; Liebert, A. Multi-wavelength time-resolved NIRS measurements for estimation of absolute concentration of chromophores: Blood phantom study. In Proceedings of the Diffuse Optical Spectroscopy and Imaging VII, Munich, Germany, 23–25 June 2019; Dehghani, H., Wabnitz, H., Eds.; SPIE: Washington, DC, USA, 2019; Volume 1107422, p. 72.
65. He, L.; Baker, W.B.; Busch, D.R.; Jiang, J.Y.; Lawrence, K.S.; Kofke, W.A.; Yodh, A.G.; He, L.; Baker, W.B.; Milej, D.; et al. Noninvasive continuous optical monitoring of absolute cerebral blood flow in critically ill adults. *Neurophotonics* **2018**, *5*, 1.
66. Durduran, T.; Yodh, A.G. Diffuse correlation spectroscopy for non-invasive, micro-vascular cerebral blood flow measurement. *Neuroimage* **2014**, *85*, 5163. [CrossRef] [PubMed]
67. Selb, J.; Zimmermann, B.B.; Martino, M.; Ogden, T.; Boas, D.A. Functional brain imaging with a supercontinuum time-domain NIRS system. In Proceedings of the Optical Tomography and Spectroscopy of Tissue X, San Francisco, CA, USA, 5–7 February 2013; Volume 8578, p. 857807.
68. Selb, J.; Joseph, D.K.; Boas, D. Time-gated optical system for depth-resolved functional brain imaging. *J. Biomed. Opt.* **2006**, *11*, 44008. [CrossRef]
69. Lange, F.; Peyrin, F.; Montcel, B. Broadband time-resolved multi-channel functional near-infrared spectroscopy system to monitor in vivo physiological changes of human brain activity. *Appl. Opt.* **2018**, *57*, 6417. [CrossRef]
70. Lange, F.; Peyrin, F.; Montcel, B. A hyperspectral time resolved DOT system to monitor physiological changes of the human brain activity. In Proceedings of the Advanced Microscopy Techniques IV and Neurophotonics II, Munich, Germany, 21–25 June 2015; OSA: Washington, DC, USA, 2015; p. 95360R.

71. Lange, F.; Dunne, L.; Tachtsidis, I. Evaluation of Haemoglobin and Cytochrome Responses During Forearm Ischaemia Using Multi-wavelength Time Domain NIRS. In *Oxygen Transport to Tissue XXXIX*; Advances in Experimental Medicine and Biology; Halpern, H.J., LaManna, J.C., Harrison, D.K., Epel, B., Eds.; Springer International Publishing: Cham, Switzerland, 2017; Volume 977, pp. 67–72. ISBN 978-3-319-55229-3.
72. Lange, F.; Tachtsidis, I. Short and mid-term reproducibility analysis of cerebral tissue saturation measured by time domain-NIRS. In Proceedings of the European Conference on Biomedical Optics, Munich, Germany, 23–25 June 2019; Volume 11074.
73. Mazurenka, M.; Jelzow, A.; Wabnitz, H.; Contini, D.; Spinelli, L.; Pifferi, A.; Cubeddu, R.; Mora, A.D.; Tosi, A.; Zappa, F.; et al. Non-contact time-resolved diffuse reflectance imaging at null source-detector separation. *Opt. Express* **2011**, *20*, 283. [CrossRef]
74. Wabnitz, H.; Mazurenka, M.; Di Sieno, L.; Contini, D.; Dalla Mora, A.; Farina, A.; Hoshi, Y.; Kirilina, E.; Macdonald, R.; Pifferi, A. Non-contact time-domain imaging of functional brain activation and heterogeneity of superficial signals. In Proceedings of the Diffuse Optical Spectroscopy and Imaging VI, Munich, Germany, 25–29 June 2017; Dehghani, H., Wabnitz, H., Eds.; SPIE: Washington, DC, USA, 2017; Volume 10412, p. 104120J.
75. Mazurenka, M.; Di Sieno, L.; Boso, G.; Contini, D.; Pifferi, A.; Mora, A.D.; Tosi, A.; Wabnitz, H.; Macdonald, R. Non-contact in vivo diffuse optical imaging using a time-gated scanning system. *Biomed. Opt. Express* **2013**, *4*, 2257. [CrossRef]
76. Di Sieno, L.; Wabnitz, H.; Pifferi, A.; Mazurenka, M.; Hoshi, Y.; Dalla Mora, A.; Contini, D.; Boso, G.; Becker, W.; Martelli, F.; et al. Characterization of a time-resolved non-contact scanning diffuse optical imaging system exploiting fast-gated single-photon avalanche diode detection. *Rev. Sci. Instrum.* **2016**, *87*. [CrossRef]
77. Torricelli, A.; Pifferi, A.; Spinelli, L.; Cubeddu, R.; Martelli, F.; Del Bianco, S.; Zaccanti, G. Time-Resolved Reflectance at Null Source-Detector Separation: Improving Contrast and Resolution in Diffuse Optical Imaging. *Phys. Rev. Lett.* **2005**, *95*, 078101. [CrossRef]
78. Dalla Mora, A.; Tosi, A.; Zappa, F.; Cova, S.; Contini, D.; Pifferi, A.; Spinelli, L.; Torricelli, A.; Cubeddu, R. Fast-Gated Single-Photon Avalanche Diode for Wide Dynamic Range Near Infrared Spectroscopy. *IEEE J. Sel. Top. Quantum Electron.* **2010**, *16*, 1023–1030. [CrossRef]
79. Contini, D.; Dalla Mora, A.; Spinelli, L.; Farina, A.; Torricelli, A.; Cubeddu, R.; Martelli, F.; Zaccanti, G.; Tosi, A.; Boso, G.; et al. Effects of time-gated detection in diffuse optical imaging at short source-detector separation. *J. Phys. D Appl. Phys.* **2015**, *48*, 045401. [CrossRef]
80. Mottin, S.; Montcel, B.; de Chatellus, H.G.; Ramstein, S.; Vignal, C.; Mathevon, N. Functional White-Laser Imaging to Study Brain Oxygen Uncoupling/Recoupling in Songbirds. *J. Cereb. Blood Flow Metab.* **2011**, *31*, 393–400. [CrossRef]
81. Ramstein, S.; Vignal, C.; Mathevon, N.; Mottin, S. In vivo and noninvasive measurement of a songbird head's optical properties. *Appl. Opt.* **2005**, *44*, 6197. [CrossRef]
82. Torabzadeh, M.; Stockton, P.; Kennedy, G.T.; Saager, R.B.; Durkin, A.J.; Bartels, R.A.; Tromberg, B.J. Hyperspectral imaging in the spatial frequency domain with a supercontinuum source. *J. Biomed. Opt.* **2019**, *24*, 1. [CrossRef] [PubMed]
83. Farina, A.; Lepore, M.; Di Sieno, L.; Dalla Mora, A.; Ducros, N.; Pifferi, A.; Valentini, G.; Arridge, S.; D'Andrea, C. Diffuse optical tomography by using time-resolved single pixel camera. In Proceedings of the SPIE BiOS, San Francisco, CA, USA, 7–12 February 2015; Tromberg, B.J., Yodh, A.G., Sevick-Muraca, E.M., Alfano, R.R., Eds.; International Society for Optics and Photonics: Bellingham, WA, USA, 2015; p. 93191K.
84. Pian, Q.; Yao, R.; Intes, X. Hyperspectral wide-field time domain single-pixel diffuse optical tomography platform. *Biomed. Opt. Express* **2018**, *9*, 6258. [CrossRef]
85. Valim, N.; Brock, J.; Niedre, M. Experimental measurement of time-dependent photon scatter for diffuse optical tomography. *J. Biomed. Opt.* **2010**, *15*, 065006. [CrossRef]
86. Zouaoui, J.; Di Sieno, L.; Hervé, L.; Pifferi, A.; Farina, A.; Mora, A.D.; Derouard, J.; Dinten, J.-M. Chromophore decomposition in multispectral time-resolved diffuse optical tomography. *Biomed. Opt. Express* **2017**, *8*, 4772. [CrossRef]
87. Di Sieno, L.; Bettega, G.; Berger, M.; Hamou, C.; Aribert, M.; Mora, A.D.; Puszka, A.; Grateau, H.; Contini, D.; Hervé, L.; et al. Toward noninvasive assessment of flap viability with time-resolved diffuse optical tomography: A preclinical test on rats. *J. Biomed. Opt.* **2016**, *21*, 025004. [CrossRef]
88. Dempsey, L.A.; Cooper, R.J.; Powell, S.; Edwards, A.; Lee, C.-W.; Brigadoi, S.; Everdell, N.; Arridge, S.; Gibson, A.P.; Austin, T.; et al. Whole-head functional brain imaging of neonates at cot-side using time-resolved diffuse optical tomography. In Proceedings of the Diffuse Optical Imaging V, Munich, Germany, 21–25 June 2015; Volume 9538, pp. 1–10.
89. Dempsey, L.A. Development and Application of Diffuse Optical Tomography Systems for Diagnosis and Assessment of Perinatal Brain Injury. Ph.D. Thesis, University College London, London, UK, 2018.
90. Jiang, J.; Ahnen, L.; Kalyanov, A.; Lindner, S.; Wolf, M.; Majos, S.S. A New Method Based on Graphics Processing Units for Fast Near-Infrared Optical Tomography. *Adv. Exp. Med. Biol.* **2017**, *977*, 191–197.
91. Arnesano, C.; Santoro, Y.; Gratton, E. Digital parallel frequency-domain spectroscopy for tissue imaging. *J. Biomed. Opt.* **2012**, *17*, 0960141. [CrossRef] [PubMed]
92. Pifferi, A.; Torricelli, A.; Bassi, A.; Taroni, P.; Cubeddu, R.; Wabnitz, H.; Grosenick, D.; Möller, M.; Macdonald, R.; Swartling, J.; et al. Performance assessment of photon migration instruments: The MEDPHOT protocol. *Appl. Opt.* **2005**, *44*, 2104–2114. [CrossRef] [PubMed]

93. Wabnitz, H.; Jelzow, A.; Mazurenka, M.; Steinkellner, O.; Macdonald, R.; Milej, D.; Zolek, N.; Kacprzak, M.; Sawosz, P.; Maniewski, R.; et al. Performance assessment of time-domain optical brain imagers, part 1: Basic instrumental performance protocol. *J. Biomed. Opt.* **2014**, *19*, 86010. [CrossRef] [PubMed]
94. Wabnitz, H.; Jelzow, A.; Mazurenka, M.; Steinkellner, O.; Macdonald, R.; Milej, D.; Zolek, N.; Kacprzak, M.; Sawosz, P.; Maniewski, R.; et al. Performance assessment of time-domain optical brain imagers, part 2: nEUROPt protocol. *J. Biomed. Opt.* **2014**, *19*, 086012. [CrossRef]
95. Quarto, G.; Pifferi, A.; Bargigia, I.; Farina, A.; Cubeddu, R.; Taroni, P. Recipes to make organic phantoms for diffusive optical spectroscopy. *Appl. Opt.* **2013**, *52*, 2494–2502. [CrossRef]
96. Wang, L.; Sharma, S.; Aernouts, B.; Ramon, H.; Saeys, W. Supercontinuum laser based double-integrating-sphere system for measuring optical properties of highly dense turbid media in the 1300–2350 nm region with high sensitivity. In Proceedings of the SPIE Photonics Europe, Brussels, Belgium, 16–19 April 2012; Volume 8427, p. 84273B.
97. Spinelli, L.; Botwicz, M.; Zolek, N.; Kacprzak, M.; Milej, D.; Liebert, A.; Weigel, U.; Durduran, T.; Foschum, F.; Kienle, A.; et al. Inter-Laboratory Comparison of Optical Properties Performed on Intralipid and India Ink. In Proceedings of the Biomedical Optics and 3-D Imaging, Miami, FL, USA, 28 April–2 May 2012; OSA: Washington, DC, USA, 2012; p. BW1A.6.
98. Aernouts, B.; Zamora-Rojas, E.; Van Beers, R.; Watté, R.; Wang, L.; Tsuta, M.; Lammertyn, J.; Saeys, W. Supercontinuum laser based optical characterization of Intralipid®phantoms in the 500–2250 nm range. *Opt. Express* **2013**, *21*, 32450. [CrossRef]
99. Aernouts, B.; Van Beers, R.; Watté, R.; Lammertyn, J.; Saeys, W. Dependent scattering in Intralipid®phantoms in the 600–1850 nm range. *Opt. Express* **2014**, *22*, 6086. [CrossRef]
100. Spinelli, L.; Botwicz, M.; Zolek, N.; Kacprzak, M.; Milej, D.; Sawosz, P.; Liebert, A.; Weigel, U.; Durduran, T.; Foschum, F.; et al. Determination of reference values for optical properties of liquid phantoms based on Intralipid and India ink. *Biomed. Opt. Express* **2014**, *5*, 2037. [CrossRef]
101. Bouchard, J.-P.; Veilleux, I.; Jedidi, R.; Noiseux, I.; Fortin, M.; Mermut, O. Reference optical phantoms for diffuse optical spectroscopy. Part 1—Error analysis of a time resolved transmittance characterization method. *Opt. Express* **2010**, *18*, 11495–11507. [CrossRef]
102. Martelli, F.; Di Ninni, P.; Zaccanti, G.; Contini, D.; Spinelli, L.; Torricelli, A.; Cubeddu, R.; Wabnitz, H.; Mazurenka, M.; Macdonald, R.; et al. Phantoms for diffuse optical imaging based on totally absorbing objects, part 2: Experimental implementation. *J. Biomed. Opt.* **2014**, *19*, 076011. [CrossRef]
103. Pifferi, A.; Torricelli, A.; Cubeddu, R.; Quarto, G.; Re, R.; Sekar, S.K.V.; Spinelli, L.; Farina, A.; Martelli, F.; Wabnitz, H. Mechanically switchable solid inhomogeneous phantom for performance tests in diffuse imaging and spectroscopy. *J. Biomed. Opt.* **2015**, *20*, 121304. [CrossRef] [PubMed]
104. Wabnitz, H.; Taubert, D.R.; Funane, T.; Kiguchi, M.; Eda, H.; Pifferi, A.; Torricelli, A.; Macdonald, R. Characterization of homogeneous tissue phantoms for performance tests in diffuse optics. In Proceedings of the SPIE BiOS, San Francisco, CA, USA, 13–18 February 2016; Volume 9700, p. 970004.
105. Xu, R.X.; Allen, D.W.; Huang, J.; Gnyawali, S.; Melvin, J.; Elgharably, H.; Gordillo, G.; Huang, K.; Bergdall, V.; Litorja, M.; et al. Developing digital tissue phantoms for hyperspectral imaging of ischemic wounds. *Biomed. Opt. Express* **2012**, *3*, 1433. [CrossRef]
106. Wabnitz, H.; Hwang, J.; Yang, L.; Macdonald, R. Digital phantom for time-domain near-infrared spectroscopy of tissue: Concept and proof-of-principle experiments. In Proceedings of the SPIE BiOS, San Francisco, CA, USA, 2–7 February 2019; p. 20.
107. Spinelli, L.; Rizzolo, A.; Vanoli, M.; Grassi, M.; Zerbini, P.E.; Pimentel, R.; Torricelli, A. Optical properties of pulp and skin in Brazilian mangoes in the 540–900 nm spectral range: Implication for non-destructive maturity assessment by time-resolved reflectance spectroscopy. In Proceedings of the International Conference of Agricultural Engineering, CIGR-AgEng2012, Valencia, Spain, 8–12 July 2012; p. C–2096.
108. Amendola, C.; Pirovano, I.; Lacerenza, M.; Contini, D.; Spinelli, L.; Cubeddu, R.; Torricelli, A.; Re, R. Use of 3D printed PLA for diffuse optics. In Proceedings of the Biophotonics Congress: Biomedical Optics 2020 (Translational, Microscopy, OCT, OTS, BRAIN), Washington, DC, USA, 20–23 April 2020; pp. 32–33.
109. Dalla Mora, A.; Martinenghi, E.; Contini, D.; Tosi, A.; Boso, G.; Durduran, T.; Arridge, S.; Martelli, F.; Farina, A.; Torricelli, A.; et al. Fast silicon photomultiplier improves signal harvesting and reduces complexity in time-domain diffuse optics. *Opt. Express* **2015**, *23*, 13937–13946. [CrossRef]
110. Martinenghi, E.; Dalla Mora, A.; Contini, D.; Farina, A.; Villa, F.; Torricelli, A.; Pifferi, A. Spectrally Resolved Single-Photon Timing of Silicon Photomultipliers for Time-Domain Diffuse Spectroscopy. *IEEE Photonics J.* **2015**, *7*, 1–12. [CrossRef]
111. Martinenghi, E.; Di Sieno, L.; Contini, D.; Sanzaro, M.; Pifferi, A.; Dalla Mora, A. Time-resolved single-photon detection module based on silicon photomultiplier: A novel building block for time-correlated measurement systems. *Rev. Sci. Instrum.* **2016**, *87*. [CrossRef] [PubMed]
112. Di Sieno, L.; Boetti, N.G.; Mora, A.D.; Pugliese, D.; Farina, A.; Konugolu Venkata Sekar, S.; Ceci-Ginistrelli, E.; Janner, D.; Pifferi, A.; Milanese, D. Towards the use of bioresorbable fibers in time-domain diffuse optics. *J. Biophotonics* **2017**, *11*, 1–12. [CrossRef] [PubMed]
113. Mora, A.D.; Di Sieno, L.; Venkata Sekar, S.K.; Farina, A.; Contini, D.; Boetti, N.G.; Milanese, D.; Nissinen, J.; Pifferi, A. Novel technologies for time-domain diffuse optics: Miniaturized wearable devices and bioresorbable optical fibers. In Proceedings of the Biophotonics Congress: Biomedical Optics Congress 2018 (Microscopy/Translational/Brain/OTS), Hollywood, FL, USA, 3–6 April 2018; p. F90-O.

114. D'Andrea, C.; Spinelli, L.; Bassi, A.; Giusto, A.; Contini, D.; Swartling, J.; Torricelli, A.; Cubeddu, R. Time-resolved spectrally constrained method for the quantification of chromophore concentrations and scattering parameters in diffusing media. *Opt. Express* **2006**, *14*, 1888. [CrossRef] [PubMed]
115. Giusto, A.; D'Andrea, C.; Spinelli, L.; Contini, D.; Torricelli, A.; Martelli, F.; Zaccanti, G.; Cubeddu, R. Monitoring absorption changes in a layered diffusive medium by white-light time-resolved reflectance spectroscopy. *IEEE Trans. Instrum. Meas.* **2010**, *59*, 1925–1932. [CrossRef]
116. Pifferi, A.; Bassi, A.; Spinelli, L.; Cubeddu, R.; Taroni, P. Time-Resolved Broadband Diffuse Spectroscopy Using a Differential Absorption Approach. In Proceedings of the Biomedical Optics and 3-D Imaging, Miami, FL, USA, 11–14 April 2010; p. BSuD45; Volume 64, p. BSuD45.
117. Yang, L.; Wabnitz, H.; Gladytz, T.; Macdonald, R.; Grosenick, D. Spatially-enhanced time-domain NIRS for accurate determination of tissue optical properties. *Opt. Express* **2019**, *27*, 26415. [CrossRef] [PubMed]
118. Yang, L.; Lanka, P.; Wabnitz, H.; Cubeddu, R.; Gladytz, T.; Konugolu Venkata Sekar, S.; Grosenick, D.; Pifferi, A.; Macdonald, R. Spatially-enhanced time-domain NIRS for determination of optical properties in layered structures. In Proceedings of the European Conference on Biomedical Optics, Munich, Germany, 23–25 June 2019; p. 9.
119. Yang, L.; Wabnitz, H.; Gladytz, T.; Sudakou, A.; Macdonald, R.; Grosenick, D. Space-enhanced time-domain diffuse optics for determination of tissue optical properties in two-layered structures. *Biomed. Opt. Express* **2020**, *11*, 6570. [CrossRef]
120. Wojtkiewicz, S.; Gerega, A.; Zanoletti, M.; Sudakou, A.; Contini, D.; Liebert, A.; Durduran, T.; Dehghani, H. Self-calibrating time-resolved near infrared spectroscopy. *Biomed. Opt. Express* **2019**, *10*, 2657. [CrossRef]
121. Kovacsova, Z.; Bale, G.; Mitra, S.; Lange, F.; Tachtsidis, I. Absolute quantification of cerebral tissue oxygen saturation with multidistance broadband NIRS in newborn brain. *Biomed. Opt. Express* **2021**, *12*, 907. [CrossRef]
122. Wabnitz, H.; Contini, D.; Spinelli, L.; Torricelli, A.; Liebert, A. Depth-selective analysis in time-domain optical brain imaging: Moments vs. time windows. *Biomed. Opt. Express* **2020**, *11*, 4224–4243. [CrossRef] [PubMed]
123. Sudakou, A.; Yang, L.; Wabnitz, H.; Wojtkiewicz, S.; Liebert, A. Performance of measurands in time-domain optical brain imaging: Depth selectivity versus contrast-to-noise ratio. *Biomed. Opt. Express* **2020**, *11*, 4348–4365. [CrossRef]
124. Lanka, P.; Yang, L.; Orive-Miguel, D.; Veesa, J.D.; Tagliabue, S.; Sudakou, A.; Samaei, S.; Forcione, M.; Kovacsova, Z.; Behera, A.; et al. The BITMAP exercise: A multi-laboratory performance assessment campaign of diffuse optical instrumentation. In Proceedings of the Diffuse Optical Spectroscopy and Imaging VII, Munich, Germany, 23–25 June 2019; Dehghani, H., Wabnitz, H., Eds.; SPIE: Washington, DC, USA; p. 44.
125. Orive-Miguel, D.; Lanka, P.; Yang, L.; Tagliabue, S.; Sudakou, A.; Samaei, S.; Veesa, J.D.; Forcione, M.; Kovacsova, Z.; Behera, A.; et al. The BitMap dataset: An open dataset on performance assessment of diffuse optics instruments. In Proceedings of the European Conference on Biomedical Optics 2019, Munich, Germany, 23–25 June 2019; p. 45.
126. Farina, A.; Pifferi, A.; Torricelli, A.; Bargigia, I.; Spinelli, L.; Cubeddu, R.; Foschum, F.; Jäger, M.; Simon, E.; Fugger, O.; et al. Multi-center study of the optical properties of the human head. In Proceedings of the Biomedical Optics 2014, Miami, FL, USA, 26–30 April 2014; Volume 6, p. BS3A.9.
127. Sordillo, L.A.; Lindwasser, L.; Budansky, Y.; Leproux, P.; Alfano, R.R. Near-infrared supercontinuum laser beam source in the second and third near-infrared optical windows used to image more deeply through thick tissue as compared with images from a lamp source. *J. Biomed. Opt.* **2015**, *20*, 030501. [CrossRef] [PubMed]
128. Yadav, J.; Rani, A.; Singh, V.; Murari, B.M. Prospects and limitations of non-invasive blood glucose monitoring using near-infrared spectroscopy. *Biomed. Signal. Process. Control* **2015**, *18*, 214–227. [CrossRef]
129. Rostami, E. Glucose and the injured brain-monitored in the neurointensive care unit. *Front. Neurol.* **2014**, *5*. [CrossRef]
130. Pinchefsky, E.F.; Hahn, C.D.; Kamino, D.; Chau, V.; Brant, R.; Moore, A.M.; Tam, E.W.Y. Hyperglycemia and Glucose Variability Are Associated with Worse Brain Function and Seizures in Neonatal Encephalopathy: A Prospective Cohort Study. *J. Pediatr.* **2019**, *209*, 23–32. [CrossRef] [PubMed]
131. Liu, J.; Zhu, C.; Jiang, J.; Xu, K. Scattering-independent glucose absorption measurement using a spectrally resolved reflectance setup with specialized variable source-detector separations. *Biomed. Opt. Express* **2018**, *9*, 5903. [CrossRef]
132. Fuglerud, S.S.; Milenko, K.; Ellingsen, R.; Aksnes, A.; Hjelme, D.R. Feasibility of supercontinuum sources for use in glucose sensing by absorption spectroscopy. In Proceedings of the European Conference on Biomedical Optics 2019, Munich, Germany, 23–25 June 2019; p. 11073_13.
133. Quarto, G.; Farina, A.; Pifferi, A.; Taroni, P.; Miniati, M. Time-resolved optical spectroscopy of the chest: Is it possible to probe the lung? In Proceedings of the European Conference on Biomedical Optics 2013, Munich, Germany, 12–16 May 2013; Taroni, P., Dehghani, H., Eds.; SPIE: Washington, DC, USA, 2013; p. 87990Q.
134. Vignal, C.; Boumans, T.; Montcel, B.; Ramstein, S.; Verhoye, M.; Van Audekerke, J.; Mathevon, N.; Van der Linden, A.; Mottin, S. Measuring brain hemodynamic changes in a songbird: Responses to hypercapnia measured with functional MRI and near-infrared spectroscopy. *Phys. Med. Biol.* **2008**, *53*, 2457–2470. [CrossRef] [PubMed]
135. Wabnitz, H.; Jelzow, A.; Mazurenka, M.; Steinkellner, O.; Macdonald, R.; Pifferi, A.; Torricelli, A.; Contini, D.; Zucchelli, L.M.G.; Spinelli, L.; et al. Performance assessment of time-domain optical brain imagers: A multi-laboratory study. In Proceedings of the SPIE BiOS, San Francisco, CA, USA, 2–7 February 2013; Volume 8583, pp. 85830L–85830L–14.

136. Ferocino, E.; Di Sciacca, G.; Di Sieno, L.; Dalla Mora, A.; Pifferi, A.; Arridge, S.; Martelli, F.; Taroni, P.; Farina, A. Spectral approach to time domain diffuse optical tomography for breast cancer: Validation on meat phantoms. In Proceedings of the European Conference on Biomedical Optics 2019, Munich, Germany, 23–25 June 2019; p. 11074_7.
137. Diop, M.; St. Lawrence, K. Improving the depth sensitivity of time-resolved measurements by extracting the distribution of times-of-flight. *Biomed. Opt. Express* **2013**, *4*, 447. [CrossRef] [PubMed]
138. Nachabé, R.; Evers, D.J.; Hendriks, B.H.W.; Lucassen, G.W.; van der Voort, M.; Rutgers, E.J.; Peeters, M.-J.V.; Van der Hage, J.A.; Oldenburg, H.S.; Wesseling, J.; et al. Diagnosis of breast cancer using diffuse optical spectroscopy from 500 to 1600 nm: Comparison of classification methods. *J. Biomed. Opt.* **2011**, *16*, 087010. [CrossRef]
139. Pifferi, A.; Farina, A.; Torricelli, A.; Quarto, G.; Cubeddu, R.; Taronia, P. Review: Time-domain broadband near infrared spectroscopy of the female breast: A focused review from basic principles to future perspectives. *J. Near Infrared Spectrosc.* **2012**, *20*, 223. [CrossRef]
140. Lindner, C.; Mora, M.; Farzam, P.; Squarcia, M.; Johansson, J.; Weigel, U.M.; Halperin, I.; Hanzu, F.A.; Durduran, T. Diffuse optical characterization of the healthy human thyroid tissue and two pathological case studies. *PLoS ONE* **2016**, *11*, e0147851. [CrossRef]
141. Lange, F.; Tachtsidis, I. Clinical brain monitoring with time domain NIRS: A review and future perspectives. *Appl. Sci.* **2019**, *9*, 1612. [CrossRef]
142. Buttafava, M.; Martinenghi, E.; Tamborini, D.; Contini, D.; Mora, A.D.; Renna, M.; Torricelli, A.; Pifferi, A.; Zappa, F.; Tosi, A. A Compact Two-Wavelength Time-Domain NIRS System Based on SiPM and Pulsed Diode Lasers. *IEEE Photonics J.* **2017**, *9*, 1–14. [CrossRef]
143. Bérubé-Lauzière, Y.; Crotti, M.; Boucher, S.; Ettehadi, S.; Pichette, J.; Rech, I. Prospects on Time-Domain Diffuse Optical Tomography Based on Time-Correlated Single Photon Counting for Small Animal Imaging. *J. Spectrosc.* **2016**, *2016*, 1–23. [CrossRef]
144. Kaynezhad, P.; Mitra, S.; Bale, G.; Bauer, C.; Lingam, I.; Meehan, C.; Avdic-Belltheus, A.; Martinello, K.A.; Bainbridge, A.; Robertson, N.J.; et al. Quantification of the severity of hypoxic-ischemic brain injury in a neonatal preclinical model using measurements of cytochrome-c-oxidase from a miniature broadband-near-infrared spectroscopy system. *Neurophotonics* **2019**, *6*, 1. [CrossRef]
145. Lange, F.; Bale, G.; Kaynezhad, P.; Pollock, R.D.; Stevenson, A.; Tachtsidis, I. Broadband NIRS Cerebral Evaluation of the Hemodynamic and Oxidative State of Cytochrome-c-Oxidase Responses to +Gz Acceleration in Healthy Volunteers. In *Oxygen Transport to Tissue XLI*; Springer: Cham, Switzerland, 2020; Volume 1232.
146. Wu, J.; Zheng, G.; Liu, X.; Qiu, J. Near-infrared laser driven white light continuum generation: Materials, photophysical behaviours and applications. *Chem. Soc. Rev.* **2020**, *49*, 3461–3483. [CrossRef]
147. Alayed, M.; Deen, M. Time-Resolved Diffuse Optical Spectroscopy and Imaging Using Solid-State Detectors: Characteristics, Present Status, and Research Challenges. *Sensors* **2017**, *17*, 2115. [CrossRef]
148. Dalla Mora, A.; Di Sieno, L.; Re, R.; Pifferi, A.; Contini, D. Time-Gated Single-Photon Detection in Time-Domain Diffuse Optics: A Review. *Appl. Sci.* **2020**, *10*, 1101. [CrossRef]
149. Mora, A.D.; Contini, D.; Arridge, S.; Martelli, F.; Tosi, A.; Boso, G.; Farina, A.; Durduran, T.; Martinenghi, E.; Torricelli, A.; et al. Towards next-generation time-domain diffuse optics for extreme depth penetration and sensitivity. *Biomed. Opt. Express* **2015**, *6*, 1749. [CrossRef] [PubMed]
150. Renna, M.; Buttafava, M.; Behera, A.; Zanoletti, M.; Di Sieno, L.; Mora, A.D.; Contini, D.; Tosi, A. Eight-Wavelength, Dual Detection Channel Instrument for Near-Infrared Time-Resolved Diffuse Optical Spectroscopy. *IEEE J. Sel. Top. Quantum Electron.* **2019**, *25*, 1–11. [CrossRef]